JOURNAL OF GEOPHYSICAL RESEARCH, VOL. 103, NO. D6, PAGES 5943–5971, MARCH 27, 1998

Latitudinal temperature gradients and climate change

D. Rind

Goddard Space Flight Center, Institute for Space Studies, New York

Abstract. The effects of a change in the latitudinal sea surface temperature gradient are investigated in several GCM experiments. Sea surface temperatures are increased/decreased in the tropics and polar regions, with little change in the global average surface air temperature. Then the experiments are repeated with colder/warmer conditions globally. Expectations generated from these runs are compared with the resulting climate changes in a doubled CO_2 experiment and show overall agreement. Results show that the latitudinal temperature gradient governs the Hadley cell intensity, eddy energy properties, and eddy transports other than latent heat. The global mean temperature governs moisture and cloud cover, Hadley cell extent, and total rainfall. The degree of tropical and subtropical moisture changes depend on both the latitudinal gradient and the mean temperature. The Aleutian low is particularly sensitive to gradient changes, while the Icelandic low (and therefore the Greenland ice core region) is not, possibly due to orographically induced constraints in the North Atlantic. The results are then compared with paleoclimate evidence to deduce what has happened to latitudinal gradients and climate in the past. It is estimated that low-latitude temperature gradients similar to today's may have occurred in the Mesozoic and in the Little Ice Age; reduced gradients were more likely in the Pliocene, Eocene, Younger Dryas, and Last Glacial Maximum. At higher latitudes, warm climates likely had reduced temperature gradients, and cold climates increased gradients. Observed equator to pole gradients were increased in the 1980s relative to the 1950s, and the simulated climate changes consistent with observations include warming of Alaska and Asia, drying in the subtropics, and moisture variability in the United States. Assignment of causes to past latitudinal gradient changes is problematic due to uncertainties concerning CO_2 and ocean heat transports, but tentative conclusions based on this analysis support the likelihood of a future, higher-CO_2 climate exhibiting a large low-latitude gradient and ample precipitation at middle latitudes.

1. Introduction

How variable is the latitudinal temperature gradient with climate change? This question is second in importance only to the question of overall climate sensitivity. Our current inability to answer it affects everything from understanding past climate variations, and paleoclimate proxies, to projections of regional effects of future greenhouse warming [*Rind*, 1995]. For example, to understand natural climate variability, some recent attempts have focused on deciphering the cause(s) of the "Little Ice Age" cooling. One approach is to model the climate system response to various forcings and compare the results with observations [*Rind and Overpeck*, 1994]. However, we do not have good observations at lower latitudes for this time period. Was the Little Ice Age a global-scale climate phenomenon, or a change in the latitudinal temperature gradient resulting from high-latitude cooling?

While we have some idea as to the amount of cooling experienced during the Last Glacial Maximum (LGM) at high latitudes, we still do not know what happened in the tropics. The discrepancy between land and some ocean data has not yet been resolved [e.g., *Rind and Peteet*, 1985; *Rind*, 1990]. Were the tropics largely invariant, as implied by the CLIMAP (Climate: Long-Range Investigation, Mapping, and Prediction) sea surface temperature reconstructions [*CLIMAP*, 1981], or did they respond strongly and help amplify the climate response, as implied by land and some ocean data [*Guilderson et al.*, 1994; *Stute et al.*, 1995; *Colinveaux et al.*, 1996; *Beck et al.*, 1997]?

For the last few hundred thousand years, assessments of climate variations are made from polar ice cores. We have no way of knowing how representative these results are for the climate at other latitudes. Of special interest are the apparent rapid climate variations seen in the Greenland ice core [e.g., *Mayewski et al.*, 1994]; do they represent fluctuations of the whole climate system, climate changes only over Greenland, or simply isotope and dust source variations due to storm track changes, perhaps associated with changes in the latitudinal temperature gradient?

The uncertainty extends to longer time periods. During the Tertiary and Mesozoic, there is substantial evidence that high latitudes were much warmer, from the presence of semitropical vegetation types to the apparent absence of land and sea ice, especially in the earlier periods [e.g., *Vakhrameev*, 1975; *Shackleton and Boersma*, 1981; *Clark*, 1988]. Again, what happened in the tropics at these times is poorly known. The use of faunal species distribution as a sea surface temperature indicator already has uncertainties for the Pleistocene; on longer timescales, its applicability is even more debatable. Isotope reconstructions suggest cooler temperatures in the tropics during much of the last 100 million years [e.g., *Dowsett et al.*, 1994].

This paper is not subject to U.S. copyright. Published in 1998 by the American Geophysical Union.

Paper number 97JD03649.

Does this imply that the latitudinal temperature gradient was that much different, or is the reconstruction faulty [*Barron and Washington*, 1982a]?

Finally, future climate projections from different models show substantial differences in the projected latitudinal temperature response from anthropogenic greenhouse perturbations. For transient climate changes, some coupled atmosphere-ocean models show a reduction in North Atlantic Deep Water production, leading to cooling at high latitudes, at least in the North Atlantic–European sector [e.g., *Washington and Meehl*, 1989; *Manabe and Stouffer*, 1994; *Russell and Rind*, 1997]. Some models also find temperatures cool initially at high southern latitudes with increased CO_2 [*Manabe et al.*, 1990; *Russell and Rind*, 1997]. Doubled CO_2 equilibrium simulations from different atmosphere-mixed layer ocean models show different degrees of high-latitude climate warming amplification; in the GFDL model, the temperature response at high latitudes is 3–4 times that at the equator, while in the GISS model, it is only close to a factor of 2 [*Rind*, 1987a]. The regional response in these different models depends on these differences in equator-to-pole gradients, which affects the hydrologic cycle, in general, and storm energetics [*Rind*, 1987a, 1988].

An obvious goal would be to clarify gradient changes by improving the quality and geographic distribution of paleoclimate observations and the representation of physical processes, particularly convection, sea ice, and ocean circulation, in GCMs for future prediction. However, if we knew what to expect, it might be possible to infer changes in the latitudinal temperature gradient from observations already available. The purpose of this paper is to examine that possibility; this will also include a discussion of the relevance of polar ice core observations to climate changes at other latitudes. We then use the results to suggest what might be expected for future climate warming.

2. Experimental Procedure

What effects would a change in latitudinal temperature gradient have on the climate system? There are many expectations that have been voiced, ranging from an increase in surface winds when the gradient increases to an increase in Hadley cell extent when the gradient decreases. However, there has been little systematic study of the detailed climate response to a gradient change. We ourselves have addressed this issue in several different publications but always in the context of global climate changes, for example the effect of different gradients in the doubled CO_2 climate [*Rind*, 1987a], or in paleoclimates [*Rind*, 1986; see also *Barron and Washington*, 1982b]. The climate change itself provided an overlay on the temperature gradient change, somewhat obscuring its direct effect. In order to address the gradient influence directly, it is necessary to change the gradient in such a way as to keep the global mean surface temperature unchanged.

Another question concerns the dependency of the results on the magnitude of temperature gradient change. Considering the nonlinear response of certain features of the climate system, especially water vapor, it is conceivable that slight changes in gradient will have very different effects from larger changes. For the same reasons, it is also possible that increases and decreases of the gradient, even if they have the same magnitude, will not produce inverse ("antisymmetrical") results.

To address these issues a series of experiments have been performed with a new version of the GISS general circulation model (GCM). The model has $4° \times 5°$ horizontal resolution, with nine vertical levels. It is essentially that described by *Rind and Lerner* [1996] (called SIM in the publication) and is similar to the version that has been tested in AMIP simulations [*Phillips*, 1994] from which many comparisons with observations are available. A recent publication evaluated the model as ranking fifth out of 28 GCMs in its ability to simulate components of the hydrologic cycle [*Lau et al.*, 1996].

Starting from a basic current climate control run, the following experiments were run: In the first experiment, sea surface temperatures were increased uniformly by 3°C in the tropics and decreased by 6°C at high latitudes, with a linear change in-between. In experiment 2 the reverse changes were applied: cooling of 3°C in the tropics and warming of 6°C at high latitudes. The resulting zonal average surface air temperature changes are shown in Figure 1. Sea ice was not altered in either experiment; therefore the main effect of changes in sea surface temperatures in sea ice regions occurs via fluxes in the prescribed sea ice leads. The changes were applied in such a way as to minimize the global surface air temperature perturbation (which would have been much more difficult had sea ice been altered [*Rind and Chandler*, 1991; *Rind et al.*, 1995]). Therefore the model response in these experiments is independent of any notable "climate" change, which is usually defined as a variation of the global mean surface temperature.

To compare these results to paleoclimate situations in which the global mean temperatures likely did change, two additional experiments were performed. In experiment 3 the increased gradient of experiment 1 was utilized, but in addition, sea surface temperatures were reduced by 4°C at all latitudes. This is in accordance with the general perception that in colder climates the gradient increases (e.g., Last Glacial Maximum). In experiment 4 the reduced gradient of experiment 2 was combined with a sea surface temperature increase of 4°C at all latitudes, in the belief that warmer climates have a reduced gradient (e.g., Mesozoic and early Tertiary climates). In both of these runs, sea ice was changed when the sea surface temperatures were above/at the freezing point. The surface air temperature change resulting from these experiments is also shown in Figure 1.

Finally, by altering the sea surface temperatures without altering climate forcing, we are in effect changing the ocean heat transports. A relevant question is whether a change in temperature gradient produced by some other mechanism, for example radiative forcing, would result in the same dynamical response. For example, land/ocean temperature contrast is altered when the sea surface temperatures are changed, introducing a longitudinal variability which may differ from that generated by other forcing mechanisms. To investigate this issue, we compare the results with the simulation of the equilibrium doubled CO_2 climate using the same model and keeping the ocean heat transports unchanged (the "q-flux" approach).

Each experiment and control run were integrated for six model years, with results shown for the last 5 years (which, by comparison with 10 year averages, produce representative results when specified sea surface temperatures are used), except for the doubled CO_2 results, which are the last 20 years of a 50 year experiment with variable sea surface temperatures. Significance is judged on the basis of 5 year interannual standard deviations.

3. Results of Altering the Latitudinal Temperature Gradient With No Global Temperature Change

3.1. Global Changes

Overall, the latitudinal mean surface air temperature gradient between the equator and the north pole was 49.3°C in experiment 1, 45.9°C in the control, and 42.1°C in experiment 2. Therefore the difference between experiment 2 and the control run shows the effect of an increase in latitudinal temperature gradient of 3.8°C, or about 8%. The gradient difference between experiments 2 and 1, of 7.2°C, represents an increase of close to 16%. Therefore we can test the influence of different magnitudes of the gradient change with these experiments. Conversely, comparing them in reverse provides an assessment of varying decreases in the gradient. Comparing each experiment to the control run (as shown in Figure 1) indicates how antisymmetric the changes are, i.e., whether a decrease and an increase provide precisely the opposite effects.

The mean value of the annual gradient change between each experiment and the control (3.6°C) is substantial. To put this in perspective, the reduction in gradient between the doubled CO_2 experiment and the control run at GISS was 3.7°C; the increase in gradient between the LGM simulation and the control run was 3.9°C. One difference, however, as shown in Figure 1, is that the tropical response in surface air temperature is about as large as that at high latitudes on the annual average (due to the unchanging sea ice and, in the northern hemisphere, large land/ocean ratio) and of opposite sign. In the previous simulations of other climates the tropical response was considerably less than that at high latitudes, especially in the LGM experiment using *CLIMAP* [1981] sea surface temperature reconstructions, and generally of the same sign. To produce changes of opposing sign would require a forcing such as a change in ocean heat transports, with a net convergence or divergence at high latitudes and the opposite at low latitudes [e.g., *Rind and Chandler*, 1991], implied by the (somewhat questionable) isotopic evidence for portions of the Cenozoic.

The surface air temperature is relatively similar in the control and in experiments 1 and 2 (Table 1); the slight differences will not affect these conclusions. This similarity is the product of the global average invariant sea surface temperature specification. The vertically integrated atmospheric temperature, less constrained, does vary somewhat, being warmest in experiment 1 with the largest latitudinal temperature gradient. The altitudinal profile of zonal average temperature differences between experiments 1 and 2 (Plate 1) indicates that the greatest difference in tropical temperatures occurs at high levels, but it is significant throughout the troposphere, while the cooler high-latitude temperatures are more confined to the low and middle troposphere. Therefore warming predominates on the vertical average. The lapse rate is reduced by about 10% in experiment 1 compared to experiment 2 (Table 1), as the moist adiabatic value is lowered with more moisture in the warmer tropics, and colder temperatures occur near the surface at high latitudes. These changes are approximately linear with the change in gradient and hence antisymmetrical relative to the control run in the two experiments.

The global average cloud cover is slightly larger in experiment 2, due primarily to an increase in middle-level clouds. This is driven by a change in the depth of convection. The experiment with the warmest tropical sea surface temperatures has more convection penetrating to the highest levels where high cloud cover increases. In experiment 2, with the coldest tropical temperatures, convection peaks at lower (midtropospheric) levels, as does moisture deposition and the resulting cloud cover. The atmospheric albedo varies in response to both cloud cover and cloud optical thickness (cloud water) changes, the latter especially important for upper level tropical clouds with the increased gradient. The slight increase in global average atmospheric albedo in experiment 1 is due to the cloud water effect (Table 1).

With an increased gradient and warmer tropical tempera-

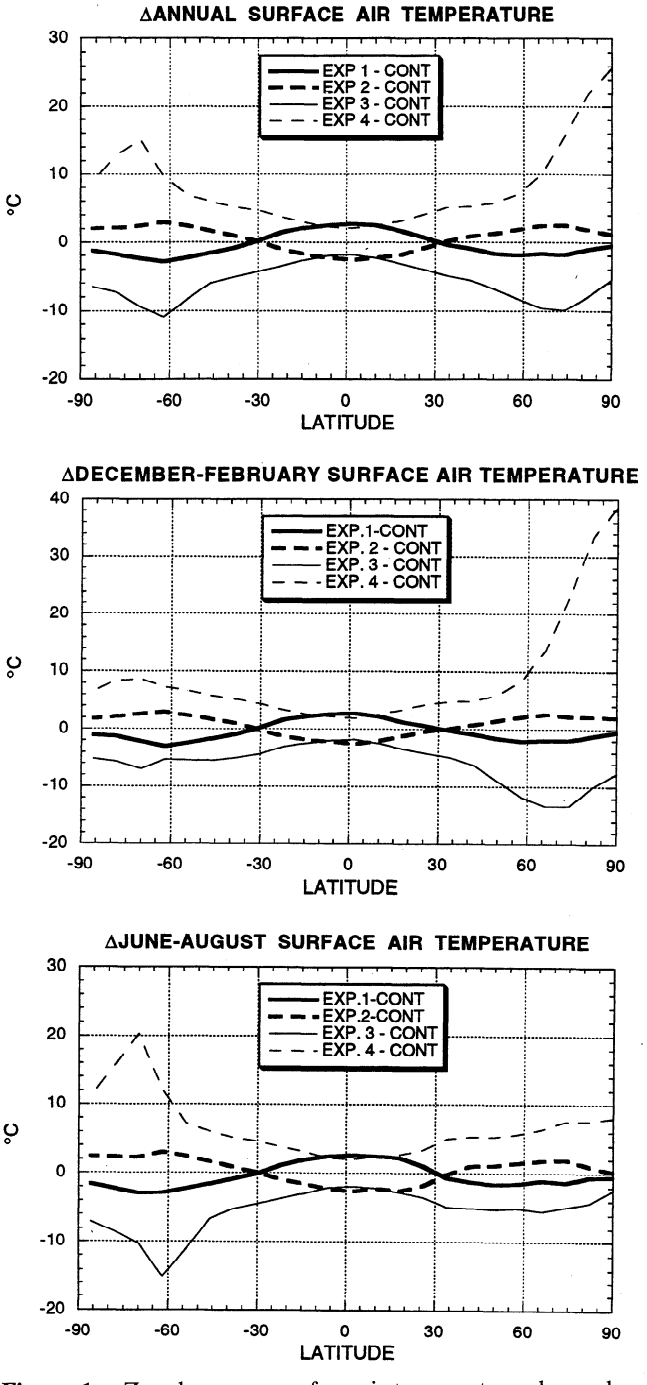

Figure 1. Zonal average surface air temperature change between the experiments and the control run for the annual average and two solstice seasons. Results are 5 year averages.

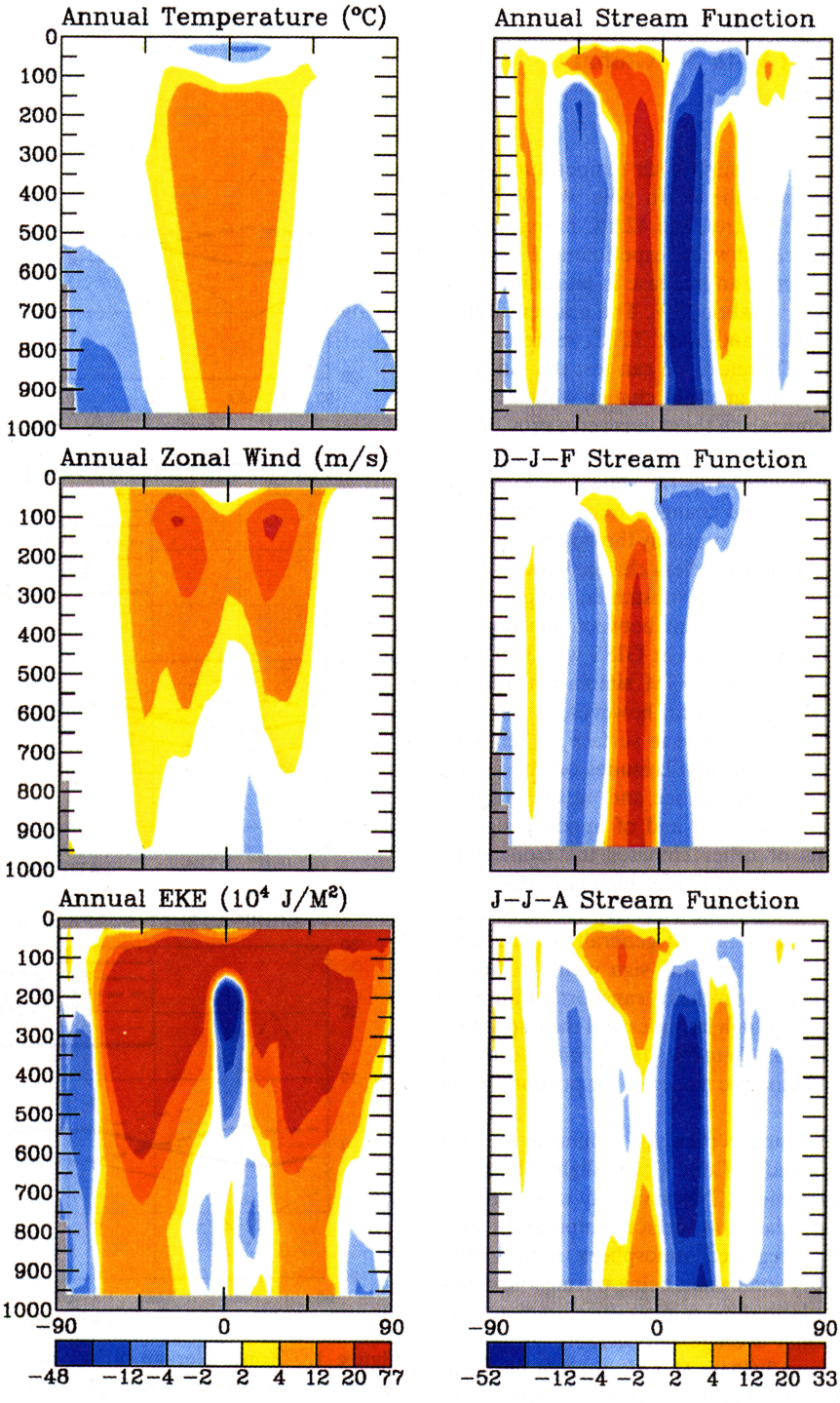

Plate 1. Change in annual average temperature (top left), wind (middle left), and eddy energy (bottom left). On the right is the change in the meridional stream function normalized by the interannual standard deviation from the control run; negative values indirect a clockwise circulation in the plane of the figure. Results are shown for the annual average and two solstice seasons.

tures, and warmer vertically integrated temperatures, global average water vapor is largest in experiment 1. As would be expected from the Claussius-Clapeyron relationship, the effect is nonlinear [(experiment 1 minus control) > (control minus experiment 2)]. A related question concerns upper tropospheric water vapor, whose variation in climate change situations has been questioned [*Lindzen*, 1990; *Sun and Lindzen*, 1993] and which has a big influence on outgoing longwave radiation [*Shine and Shine*, 1991]. The warmer tropics is nonlinearly associated in the model with increased water vapor in the upper troposphere (Table 1), even though the global mean surface air temperature is unchanged. Despite this added greenhouse capacity, net longwave radiation loss at the top of the atmosphere is greatest in experiment 1 due to its warmer atmospheric temperatures.

Rainfall is reduced in experiment 2, with the cooler tropical temperatures (Table 1), as is evaporation (latent heat flux); surprisingly, the global average effects are linear. The rainfall

Table 1. Global, Annual Average Quantities for Various Experiments and Control Runs

Parameter	Units	Cont.	Exp. 1	Exp. 2	Exp. 3	Exp. 4	$2 \times CO_2$	Cont. $2 \times CO_2$	s.d.
Surface temperature	°C	13.8	13.9	13.6	8.8	19.0	17.39	13.88	0.025
Sea surface temperature	°C	19.2	19.2	19.2	17.6	22.3	21.7	19.4	0
Air temperature	°C	−23.6	−22.3	−24.7	−27.2	−18.2	−20.3	−23.5	0.025
Lapse rate	°C km^{-1}	6.01	5.74	6.23	5.90	6.09	5.87	6.01	0.005
Planetary albedo	%	31.07	31.45	30.68	32.45	29.15	30.78	30.92	0.056
Ground albedo	%	13.1	13.4	12.7	17.4	6.41	11.8	12.3	0.037
Atmospheric albedo	%	27.2	27.6	27.0	26.5	28.5	27.9	27.5	0.064
Cloud cover	%	56.4	55.8	57.1	55.7	61	56.5	56.7	0.016
High clouds	%	14.0	13.7	13.5	11.9	15.8	15.7	14.3	0.07
Low clouds	%	46.6	46.1	46.8	46.4	46.2	46.0	46.9	0.15
Cloud water	ppmm	10.8	11.8	10.0	10.0	11.6	11.9	11.0	0.05
Atmospheric water vapor	mm	22.9	25.2	21.3	17.7	30.5	29.7	23.4	0.04
Upper tropospheric water vapor (above 550 mbar)	ppmm	1180	1507	978	821	1795	2032	1213	12
Net shortwave radiation at top	W m^{-2}	232.7	231.4	234.0	228	234.6	233.7	233.2	0.16
Net longwave radiation at top	W m^{-2}	−232.3	−233.5	−231.1	−226	−238.8	−233.8	−233	0.14
Net radiation at top of atmosphere	W m^{-2}	0.3	−2.1	2.9	2.0	−4.2	−0.1	0.2	0.11
Sensible heat	W m^{-2}	−24.0	−24.5	−23.5	−26.1	−21.6	−21.4	−23.8	0.15
Latent heat	W m^{-2}	−91.7	−93.3	−90.2	−81.0	−103.7	−99.6	−93.1	0.20
Net heat at surface	W m^{-2}	−0.33	−2.89	2.54	1.30	−4.51	−0.38	−0.42	0.15
Precipitation	mm d^{-1}	3.17	3.22	3.12	2.80	3.58	3.44	3.22	0.007
Snow cover	%	10.8	11.3	10.4	19.1	5.8	9.3	11.5	0.04
Sea ice cover	%	3.9	3.9	3.9	10.9	0	2.7	4.1	0

decrease in experiment 2, along with its warmer temperatures at high latitudes, results in less snow cover, and thus ground albedo is reduced (sea ice is fixed). The planetary albedo change, driven by the ground albedo and cloud cover differences, produces less net shortwave radiation absorption with the largest gradient (Table 1).

Therefore experiment 1 loses the most longwave radiation and absorbs less shortwave radiation. Both the net radiation at the top of the atmosphere and the net heating at the surface indicate that were the sea surface temperatures allowed to adjust, the experiments would not have maintained the same global mean temperature; experiment 1 would have cooled, and experiment 2 would have warmed. Given the model's sensitivity of 3.5° for a doubled CO_2 forcing of 4 W m^{-2}, or about 0.875°C/W m^{-2}, experiment 1 would have cooled by ~1.75°C, while experiment 2 would have warmed by ~2.8°C. Given the distributions shown in Figure 1, it is likely that these changes would have occurred in the tropics, despite the greater/lesser water vapor greenhouse capacity there in experiment 1/experiment 2. Clearly, the model's atmosphere does not have the capability of rearranging its radiative constituencies to accommodate this change in gradient with the current atmospheric composition. The oceans implicitly have had a change in ocean heat transports to produce the altered sea surface temperature gradient; therefore even in the best situation, with the model's ocean forcing able to sustain this altered ocean transport, the radiative imbalance would still not allow the gradient to be maintained. As discussed by *Rind and Chandler* [1991], allowing sea ice to vary can result in a stable change in temperature gradient with the current atmospheric composition, although with a net change in global average temperature.

3.2. Hydrologic Cycle

With an increased gradient the tropical precipitation increases, and subtropical precipitation decreases (Figure 2). The effect occurs in both winter and summer, but the subtropical effect tends to be largest in summer. The effect is also somewhat nonlinear; as the gradient is increased further, the changes are larger. The opposite tendencies at tropical/subtropical latitudes help explain the linear response of the global precipitation to the gradient change.

Latent heat release associated with the precipitation change helps drive the Hadley cell. Therefore consistent with the precipitation result, the Hadley cell originating from the equator intensifies with the larger gradient. Plate 1 shows (right) the difference between the two experiments normalized by the standard deviation. Again, the effect is greater in the summer hemisphere. The differences are large, peaking in the winter hemisphere at 25–50% in the northern hemisphere (NH) and at greater than 50% in the southern hemisphere (SH). In the summer hemisphere the differences are so large that the circulation cell actually changes sign. The precipitation increases in the tropics are associated with increased vertical velocities, while the decreases are associated with increased subsidence (Figure 3). Note that in the model, globally averaged upper tropospheric water vapor is increasing despite the increase in Hadley cell intensity and subtropical subsidence, in contrast to the argument of *Sun and Lindzen* [1993].

Rind and Rossow [1984], from a series of GCM experiments, concluded that the Hadley circulation is driven by two competing heating sources which are not in phase during the solstices: solar radiation, peaking at 23° latitude, and latent heat release, driven by equatorial precipitation. In the summer hemisphere the two sources are actually in conflict, inciting circulation cells between 0° and 23° latitude of opposite direction. With an increase in latitudinal temperature gradient and gradient of latent heat release, the solar heating source is overwhelmed, and the circulation changes sign; hence a greater effect occurs in the summer hemisphere.

Associated with the vertical velocity changes are variations in cloud cover (Figure 4), with high cloud cover tracking the vertical motion at low and subtropical latitudes. Low clouds are affected in the extratropics due to an eddy energy and moisture availability increase in experiment 1. Midlatitude

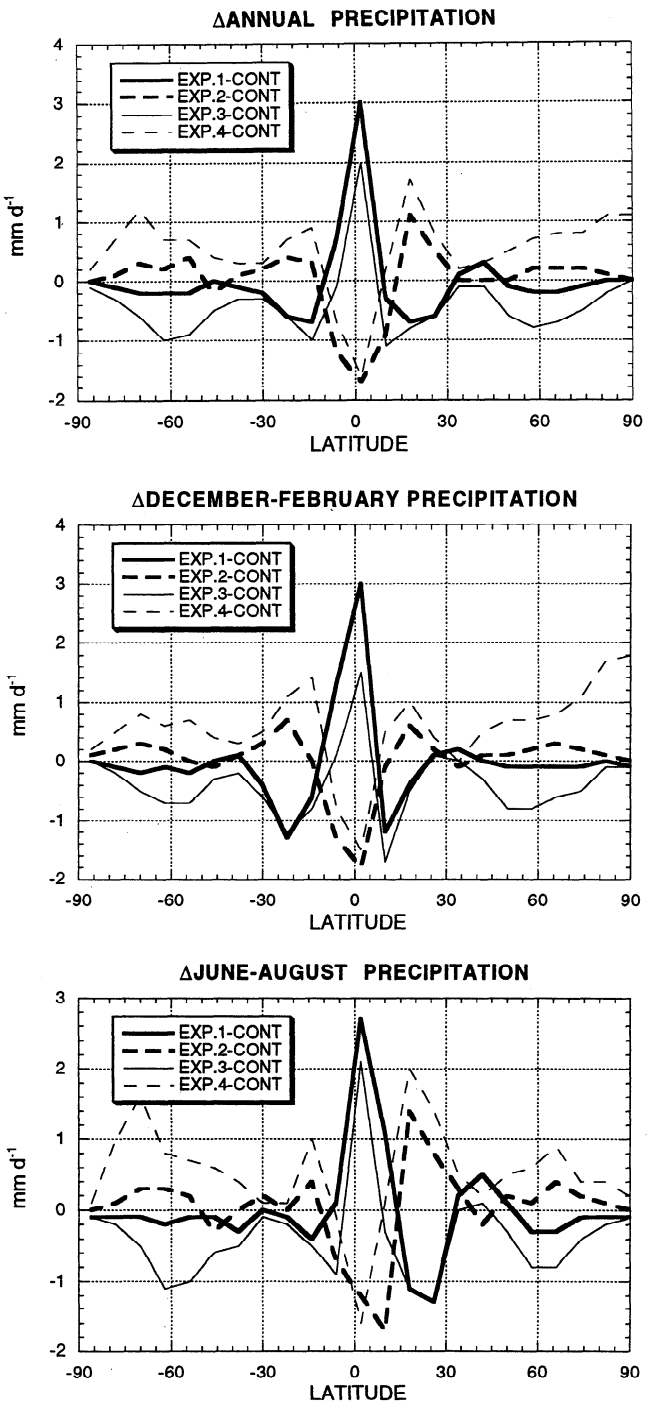

Figure 2. As in Figure 1 except for precipitation.

high-level clouds are underestimated in the control run, and therefore their change is less reliable. Planetary albedo changes provide for decreased solar absorption at the surface with the increased gradient, a negative feedback which would have an effect if the sea surface temperatures were not specified.

Other elements of the hydrologic cycle will also change, and the net effect on soil moisture depends on the difference between the changes of precipitation, evaporation, and runoff. The changes over land in precipitation, precipitation minus evaporation, and soil moisture in the subtropics are of opposite sign in the two experiments (Figure 5). In experiment 2 the tropics are dry; experiment 1 shows little change, in contrast to the results given in Figure 2 averaged over both land and ocean. The warmer tropical sea surface temperatures in experiment 1 lead to more oceanic precipitation which results in a circulation cell of rising marine air, and subsidence over the tropical land, minimizing its response. These results are summarized in Table 2.

The change in gradient does not produce large impacts on the poleward extent of the Hadley circulation in the northern hemisphere. By interpolating the location of the vertically integrated value, it appears as if in the southern hemisphere the reduced gradient results in a slight extension of Hadley cell subsidence poleward (Table 2).

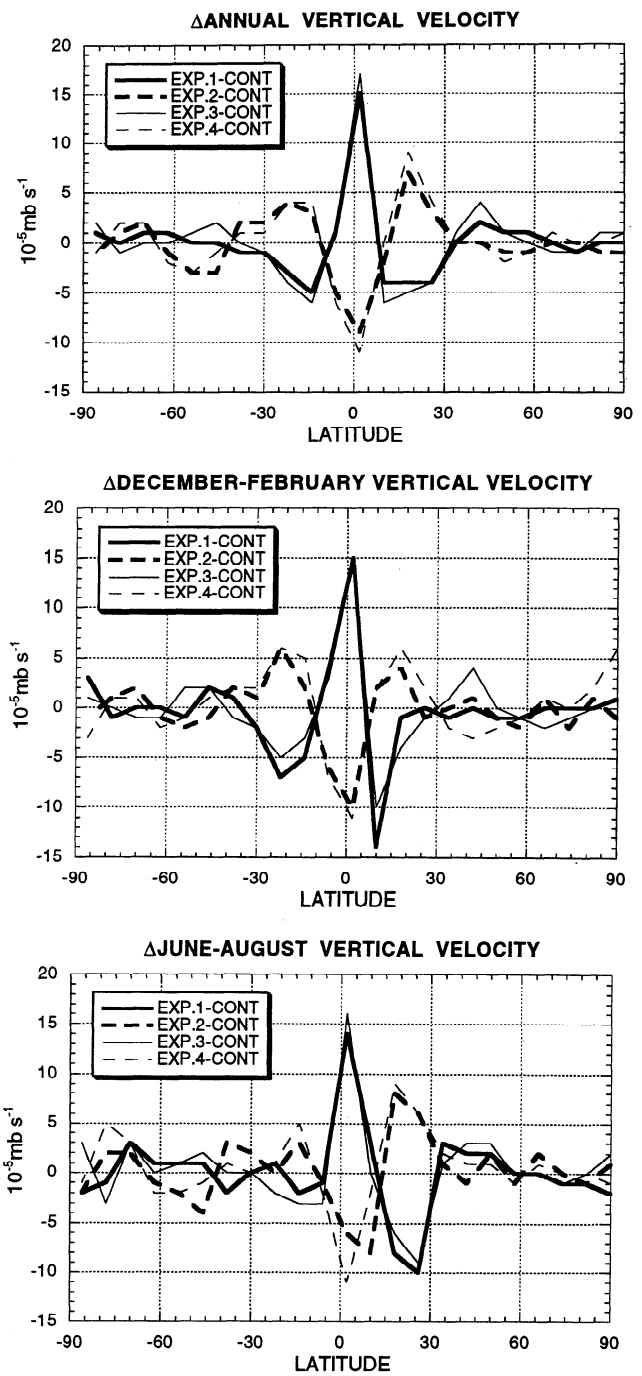

Figure 3. As in Figure 1 except for the negative of vertical velocity (positive values indicate upward flow).

3.3. Eddy Energy and Transports

There are strong expectations as to how eddies should respond to an increased temperature gradient. Since baroclinic processes which provide the predominant portion of eddy energy are directly related to the latitudinal temperature gradients, eddies should become more active when that gradient increases. Furthermore, the wavelength of maximum baroclinic instability should become larger with an increased temperature gradient [*Kuo*, 1952], and eddy transports should likewise increase.

Eddy energy increases outside of the tropics with the increase in gradient (Plate 1), although the effect is larger in the middle to upper troposphere than it is nearer the surface. The latitudinal temperature gradient is larger at all levels; the larger response at higher levels is due to increased vertical propagation of eddy energy from low levels with the increased gradient [see *Rind*, 1987a]. In the tropics, warmer temperatures result in increased convection, leading to increased momentum mixing by convection, which destroys eddy energy.

It is generally believed that standing eddies are generated by interaction with the topography and land/ocean contrast, thus are less sensitive to the latitudinal temperature gradient than are transient eddies; standing eddies may, in fact, help control the gradient. However, the ratio between the standing and the

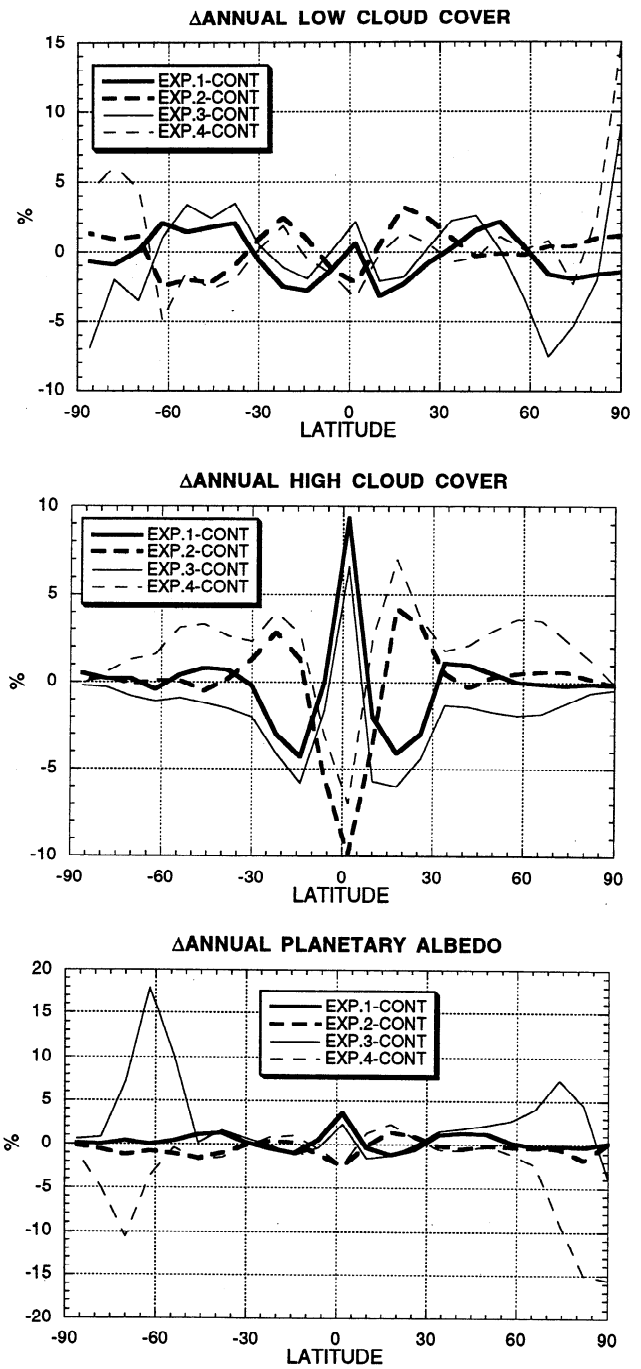

Figure 4. Annual average change between each experiment and control for low clouds (top), high clouds (middle), and planetary albedo (bottom).

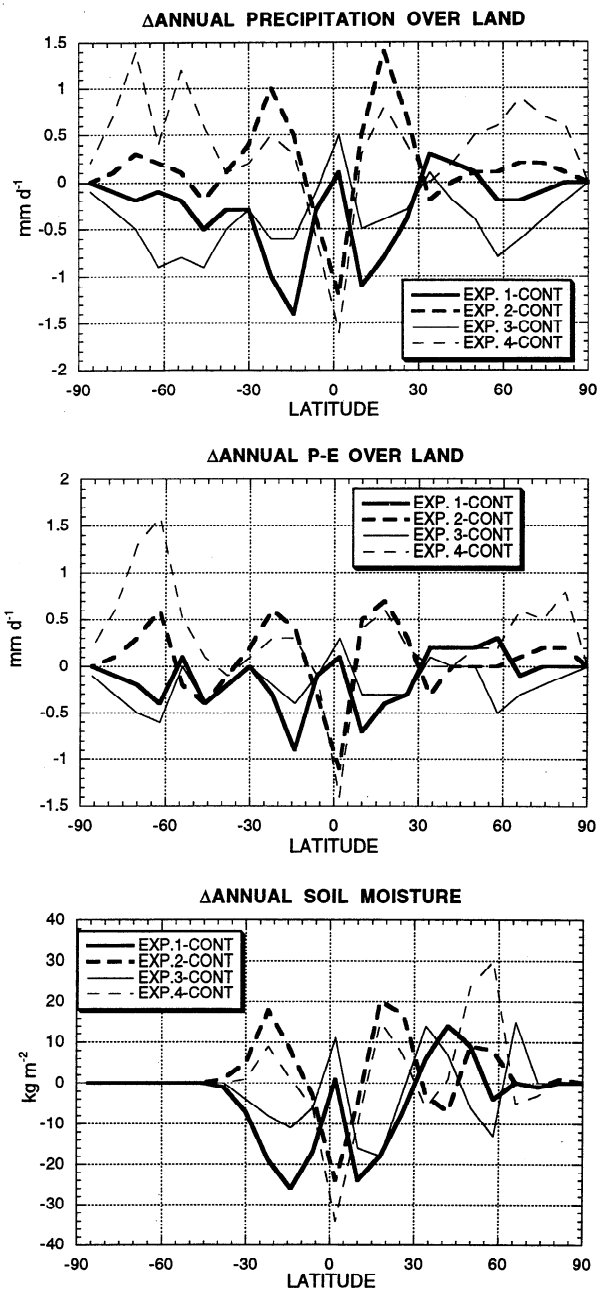

Figure 5. Annual average change in precipitation over land (top), precipitation minus evaporation over land (middle), and soil moisture (bottom) between each experiment and the control run.

Table 2. Hydrologic and Hadley Cell Characteristics in Different Simulations

	Cont.	Exp. 1	Exp. 2	Exp. 3	Exp. 4	Cont. ($2CO_2$)	$2 \times CO_2$
Annual precipitation 10°N–10°S (mm d^{-1})	5.6	6.7	4.2	5.8	4.9	5.5	6.0
Annual precipitation 20°N (mm d^{-1})	3.1	2.4	4.2	2.3	4.8	3.2	3.1
Annual precipitation 10°N–10°S over land (mm d^{-1})	6.5	6.0	6.1	6.4	5.8	6.4	6.4
Annual precipitation 20°N over land (mm d^{-1})	2.6	1.7	3.9	2.1	3.3	2.7	2.3
Annual P − E 10°N–10°S over land (mm d^{-1})	2.9	2.5	2.6	2.8	2.3	2.8	2.7
Annual P − E 20°N over land (mm d^{-1})	0.8	0.4	1.5	0.5	1.4	0.8	0.6
Annual soil moisture (kg m^{-2}) 10°N–10°S	317	304	307	313	300	312	312
Annual soil moisture (kg m^{-2}) 20°N	179	161	199	161	194	177	169
January peak Hadley cell (10^9 Kg s^{-1});	−158	−183	−139	−205	−128	−182	−170
Latitude of peak	8°N	8°N	16°N	8°N	8°N	8°N	8°N
January vertical velocity 2°N/18°N (10^{-5} mbar s^{-1})	13/−15	28/−16	3/−11	28/−19	2/−9	14/−15	14/−14
January poleward extent of Hadley cell	34°N	34°N	34°N	31°N	36°N	34°N	36°N
July peak Hadley cell (10^9 Kg s^{-1})	194	199	192	226	209	196	181
Latitude of peak	8°S	8°S	8°N	8°S	8°N	8°S	8°S
July vertical velocity 10°N/22°S	21/−16	24/−15	13/−16	21/−18	19/−15	19/−17	19/−16
July poleward extent of Hadley cell	32°S	32°S	33.5°S	31°S	34°S	32°S	33°S

transient eddy energy in the model showed little change. For example, in the northern hemisphere on the annual average it is 14% in the control run and 15% in both experiments 1 and 2. The southern hemisphere also shows little change. Standing energy will be affected by the flow over topography, and as discussed below, the zonal flow increases with the increased gradient.

The hemispheric average tropospheric eddy kinetic energy (EKE) increases continually with the increased gradient, but the effect is nonlinear, as experiment 1 shows a big increase (Table 3). Baroclinic generation from potential to kinetic energy (P → K) also increases with an increased gradient, while the energy lost to the zonal mean flow (KE → KZ) decreases. Hence the generation of eddy energy by the dynamics (KDYN) continually increases from experiment 2 to experiment 1. Dissipation of eddy energy by momentum mixing (KCONV) is slightly greater with the decreased gradient because while convection to the highest levels is less, overall convective mass flux is actually greater. Convection to the highest levels helps stabilize the vertical temperature profile, reducing convection in the model [*Rind*, 1986]. Surface friction (KSURF) removes more energy when the energy is greater in experiment 1.

Eddy available potential energy (EAPE) is actually larger in experiment 2, an unexpected result since it is the relationship of APE to the latitudinal temperature gradient which led to the expectation of increased eddy energy in the first place. Without this effect, the EKE change would likely have been larger; note the small change in P → K in experiment 1. EAPE transformation to kinetic energy is smaller in experiment 2, but the primary difference is associated with the greater surface forcing (PSURF) of potential energy via sensible heat release, occurring as a result of the warmer extratropical ocean temperatures; relative to the cold land in winter, the warmer extratropical oceans in experiment 2 provide for greater longitudinal temperature variability. Condensational heat release in the model plays a complex role, acting to decrease EAPE by stabilizing the vertical temperature gradient, while at the same time, increasing local temperature gradients by maximizing in warm air. Apparently, the net effect of condensation (PCOND) is more negative as the gradient is reduced. Loss of EAPE by radiation (PRAD) is greatest with the warmer extratropics, while the gain by the sea level pressure filter (PFIL), used in the model, is similar in the different simulations.

What happens to the change in wavelength of the eddies? As noted above, one would expect from baroclinic considerations that with a larger gradient, generation would shift to longer wavelengths, at least from linear, small-amplitude wave theory. Globally, the largest increase in baroclinic generation occurs for wavenumber 5; this represents a slight shift to long wavelengths, since the control run global average peak generation is in wavenumber 6. Peak changes in eddy energy generally occur in zonal wavenumbers 3–5 in the different hemispheres (Figure 6). More energy overall is located in wavenumbers 1 and 2, but as seen in the figure, there is less change in their energy, especially in the northern hemisphere. It may be argued that in this hemisphere the longest waves are more affected by orography, land/ocean configuration and contrast, and hence less susceptible to latitudinal temperature gradient influences; wavenumbers 1 and 2 do have the highest proportion of standing wave energy in the model. The phase of standing wavenumbers 3–5 is also altered somewhat; for example, at middle latitudes, wavenumber 3 is some 20° farther west with the increased gradient, and wavenumber 4 is 15° farther east. However, these are relatively small changes, and since the time-

Table 3. Annual Northern Hemisphere Tropospheric Eddy Energy (10^{17} J) and Sources/Sinks (10^{12} W)

Run	EKE	EAPE	P-K	KE-KZ	KDYN	KCONV	PCOND	PRAD	KSURF	PSURF	PFIL
Cont.	1377	5774	550	−160	390	−110	−455	−244	−281	769	101
Exp. 1	1536	5569	553	−148	405	−106	−289	−210	−300	619	104
Exp. 2	1292	6180	541	−167	374	−117	−577	−297	−257	959	103
Exp. 3	1531	5809	585	−165	420	−104	−336	−249	−316	655	100
Exp. 4	1231	5736	500	−146	354	−117	−557	−226	−237	947	106
Cont. $2 \times CO_2$	1402	5877	574	−162	392	−109	−490	−249	−283	823	109
$2 \times CO_2$	1350	5531	541	−157	384	−110	−425	−206	−274	680	105

average appearance of the middle troposphere features three troughs, the main effect of the increased gradient is to amplify the current trough/ridge structure while maintaining the same general configuration.

The results are definitely not linear or antisymmetric. As shown in Figure 6, as the gradient gets stronger (experiment 1 minus control), wave 3 shows more of a response. Hence the basic idea that longer waves will be amplified with an increased gradient is verified, although the effect does not maximize at the longest wavelengths.

Evident in both Table 3 and Figure 6 for eddy energy, in general, is that bigger increases occurred in experiment 1 relative to the control than for the control relative to experiment 2. This effect is associated primarily with a reduction in the loss of energy to the zonal mean flow in experiment 1. Jet stream level winds increase with an increase in the gradient (consistent with the thermal wind relationship), while in the tropics, the effect of the stronger Hadley circulation appears as an increase in low-level east winds (Plate 1). The differences in each experiment are relatively similar in magnitude, but kinetic energy is a function of wind velocity squared, so the zonal kinetic energy (ZKE) is much larger in experiment 1. Global tropospheric ZKE increases by 623×10^{17} J (22%) from experiment 2 to the control run and by 846×10^{17} J (30%) from the control run to experiment 1. Apparently, as the zonal kinetic energy increases, there is less net energy transfer from eddies; the additional kinetic energy is coming directly from transformation of zonal available potential energy (ZAPE) to ZKE, i.e., by the stronger Hadley cell. With the increased gradient, ZAPE is larger by 8300×10^{17} J, or 30% in experiment 1 compared to experiment 2.

It is often expected that surface winds would increase with a stronger latitudinal temperature gradient. Consistent with this expectation, and the overall increase in ZKE, global average surface wind magnitudes increase by 14% from experiment 2 to experiment 1, with increases at almost all latitudes.

What happens to eddy and total transports? This issue has been addressed in previous climate change experiments [e.g., *Rind*, 1987a; *Manabe and Wetherald*, 1980], but the influence of the climate change obscured the latitudinal gradient change effect. With an increase in both the eddy energy and the Hadley circulation as the gradient increased, we should expect transports to increase as well. This result does occur, as shown in Figure 7, and is relatively linear, despite the various nonlinearities identified previously. With the increased gradient, eddy transport of sensible heat increases at midlatitudes (Figure 7, top), and the transport increase is greater and extends to the subtropics when latent heat is included (static energy transport) (Figure 7, middle). The total northward atmospheric transport of static energy, the result of both eddies and the mean circulation, increases at all latitudes except for the highest southern latitudes (Figure 7, bottom). At the highest latitudes the temperature gradient effects start decreasing with latitude (Figure 1), which may influence the dynamic response there.

In general, then, the atmospheric dynamics is acting to reduce the imposed sea surface temperature gradient, which implies compensation between the atmospheric and (implied) the ocean transport effect. The implied ocean heat transports can be calculated from the convergence/divergence of heat necessary to produce the specified sea surface temperatures, given the radiative, latent, and sensible heat fluxes which occurred in the model during the simulation. These implied transports are shown in Figure 8 (top). While atmospheric

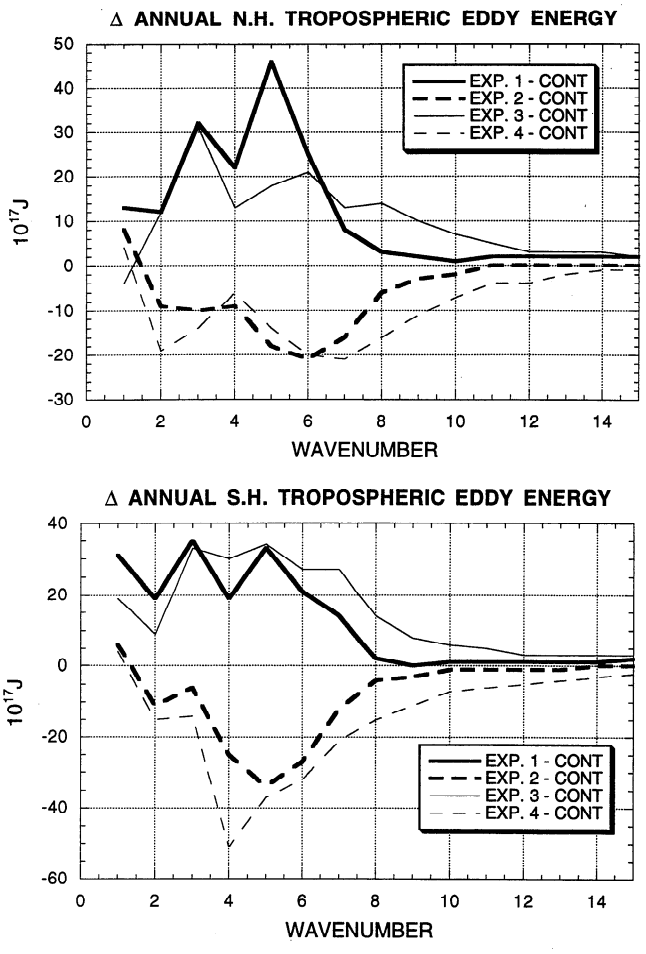

Figure 6. Annual average change in tropospheric eddy energy as a function of wavenumber between each experiment and the control run for the northern hemisphere (top) and the southern hemisphere (bottom).

transports were greater in experiment 1, poleward ocean heat transports are greater in experiment 2, as they are needed to reduce the latitudinal temperature gradient. The results are fairly symmetrical, indicating that the net heating at the ocean surface is approximately linear with temperature change.

An exact compensation does not occur in the total change in atmospheric plus oceanic energy transport (Figure 8, bottom), although the changes are relatively small. In the control run, atmospheric transports peak at approximately 4×10^{15} W in middle latitudes, with values one quarter as large in the tropics and high latitudes. The implied ocean transports peak at $\sim 2 \times 10^{15}$ W in the subtropics, dropping to one-third that value at 60° latitude. With this perspective, the change in total energy transports is generally of the order of 5% relative to the control run in the southern hemisphere and less in the northern hemisphere. The differences at low latitudes between the two experiments are at most 10% of mean values, with little consistent change with increased gradient.

3.4. Regional Changes

The various larger-scale changes have implications for regional effects. Because the significance grows as the gradient change increases, we concentrate here on the difference between experiments 1 and 2. The degree of nonlinearity experienced can be estimated from the results discussed previously.

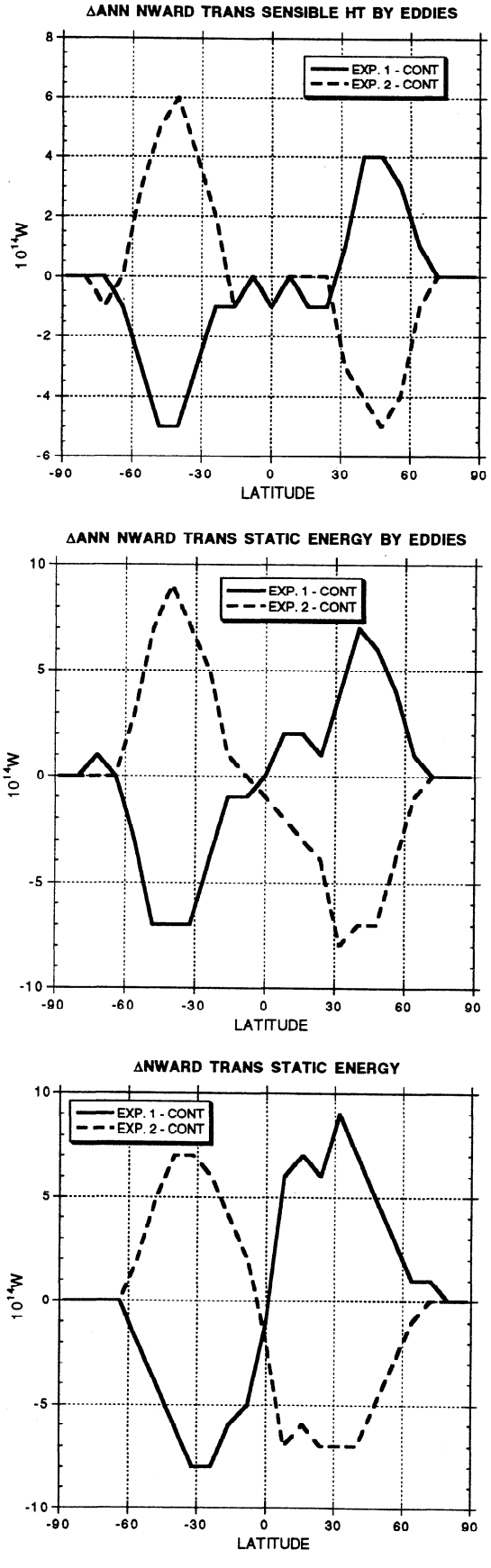

Figure 7. Change in annual northward eddy transport of sensible heat (top) and static energy (middle) between experiments 1 and 2 and the control run. Also shown is the change in total atmospheric static energy transport (bottom).

The specification of sea surface tropical warming and high-latitude cooling with the increased gradient results in surface air temperature differences which mimic the input ocean temperatures (Plate 2). This effect is dampened inland over Eurasia where the direct marine influence is less. In the tropics, even though it is the sea surface temperature changes that are specified, the warming is actually largest over land. High-latitude cooling is largest in the North America-North Atlantic-western Europe sector.

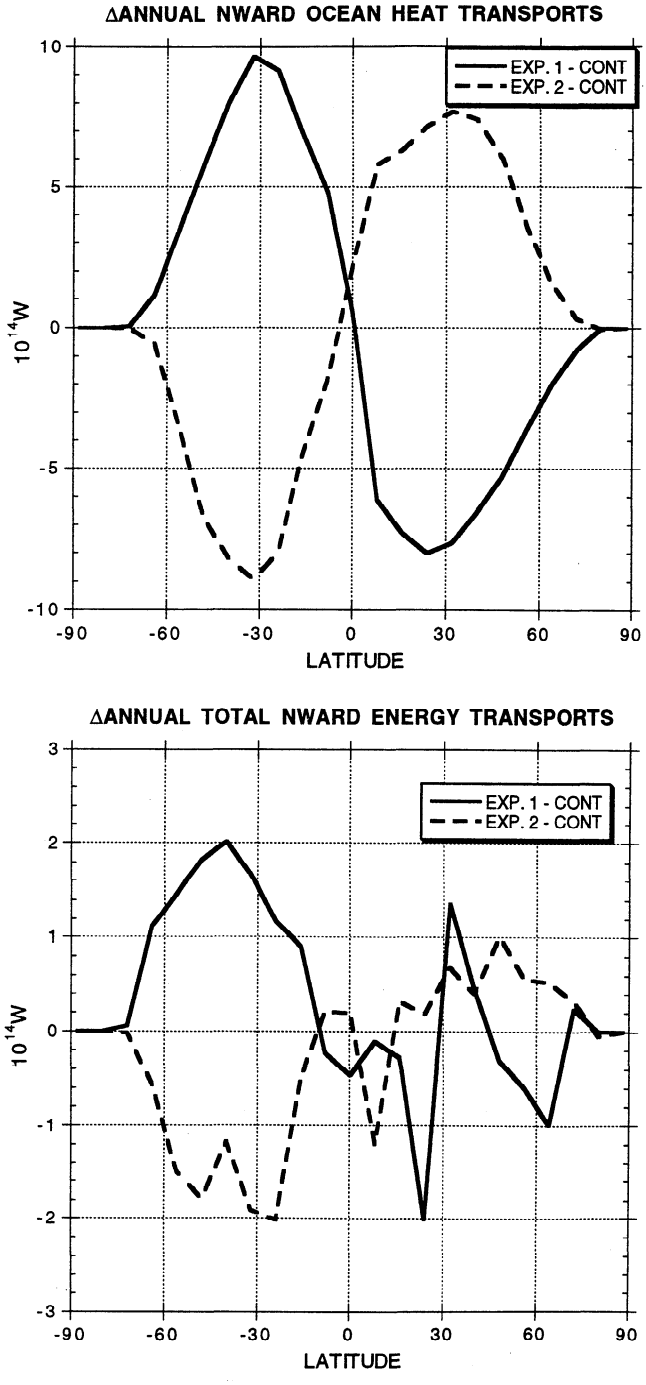

Figure 8. Change in (implied) annual northward transport of heat by the ocean (top) and total atmosphere plus ocean energy transport (bottom) between experiments 1 and 2 and the control run.

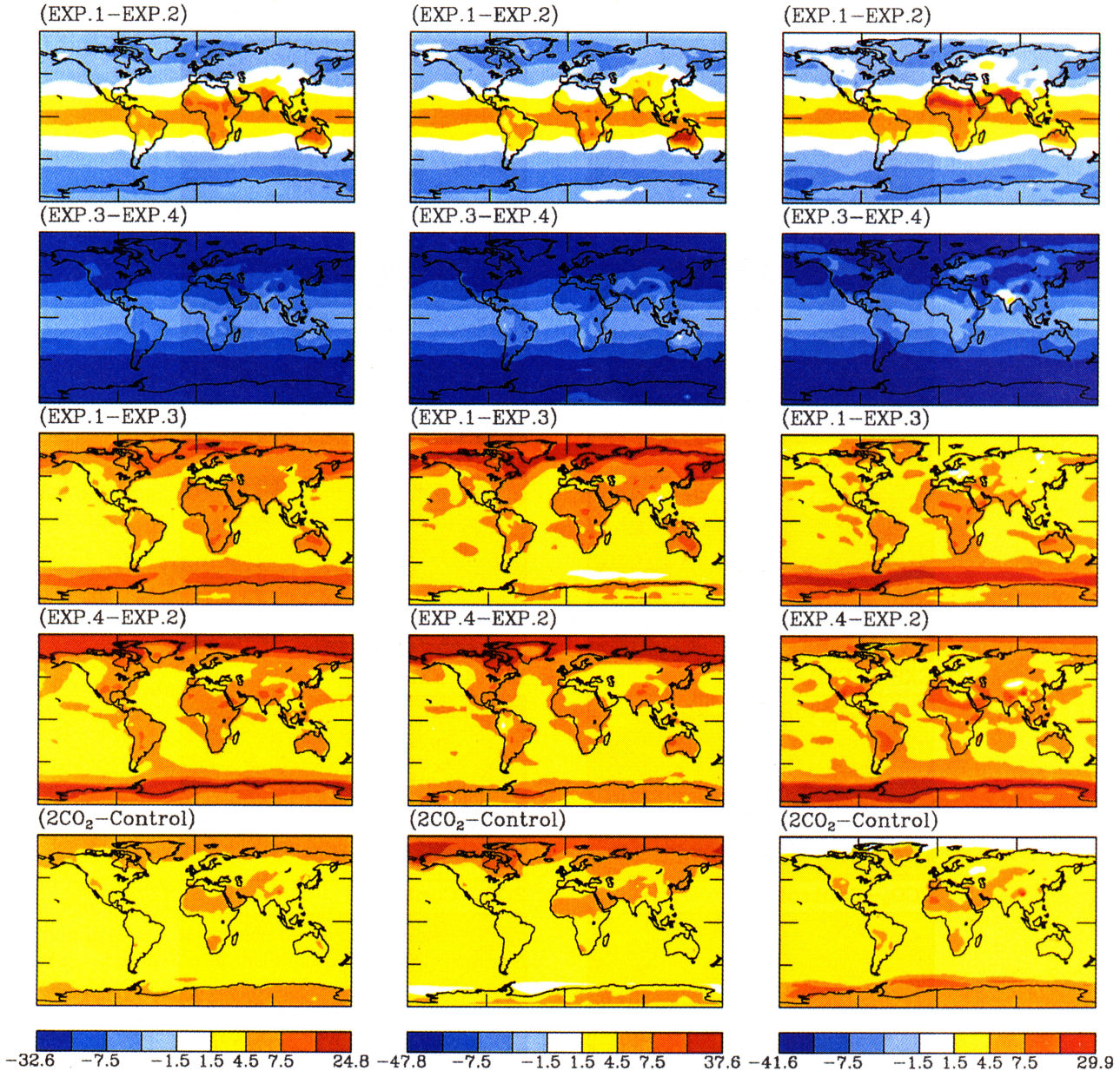

Plate 2. Geographical change in surface air temperature (°C) for the annual average (left), December–February (middle), and June–August (right). Results are shown for experiment 1 minus experiment 2 (top row), experiment 3 minus experiment 4 (row 2), experiment 1 minus experiment 3 (row 3), experiment 4 minus experiment 2 (row 4), and the change due to doubled atmospheric CO_2 (bottom row).

The local temperatures are also affected by advective changes, associated with the sea level pressure variations (Figure 9). Overall, tropical pressures decrease, while middle- and high-latitude values increase, especially in the northern hemisphere during summer. Oceanic subtropical highs are intensified primarily in the summer hemisphere, consistent with the greater Hadley cell subsidence (Figure 3). With the increased gradient the eastern portion of the Icelandic low weakens somewhat, while the southwestern portion intensifies somewhat in winter. The Aleutian low deepens in all seasons. The pattern over the North Pacific and North America looks much like the "PNA" pattern associated with El Niños, in these runs in conjunction with an increased sea surface temperature latitudinal gradient over all longitudes of the North Pacific. The pattern over the North Atlantic in winter shows an increased pressure gradient somewhat to the west of the normal occurrence of the North Atlantic Oscillation (NAO) [*Kushnir*, 1994]. Experiment 1 also has intensified winter lows around Antarctica, especially in the vicinity of the Pacific and Indian Ocean sectors.

The surface wind changes (Figure 10) associated with the increased (anticyclonic) sea level pressure tendency extend the cooling over northwestern Europe, while the return flow on the western side helps moderate Greenland cooling on the annual average. The intensified Aleutian low provides for more south winds producing warming over Alaska and cooling in northeastern Asia. Higher pressure to the south of the Aleutian low, associated with increased Hadley cell subsidence, promotes a more south to north flow in central Asia, helping to extend warming into the Tibetan region. The increased Hadley cell results in amplified trade winds. Increased cyclonic circulation

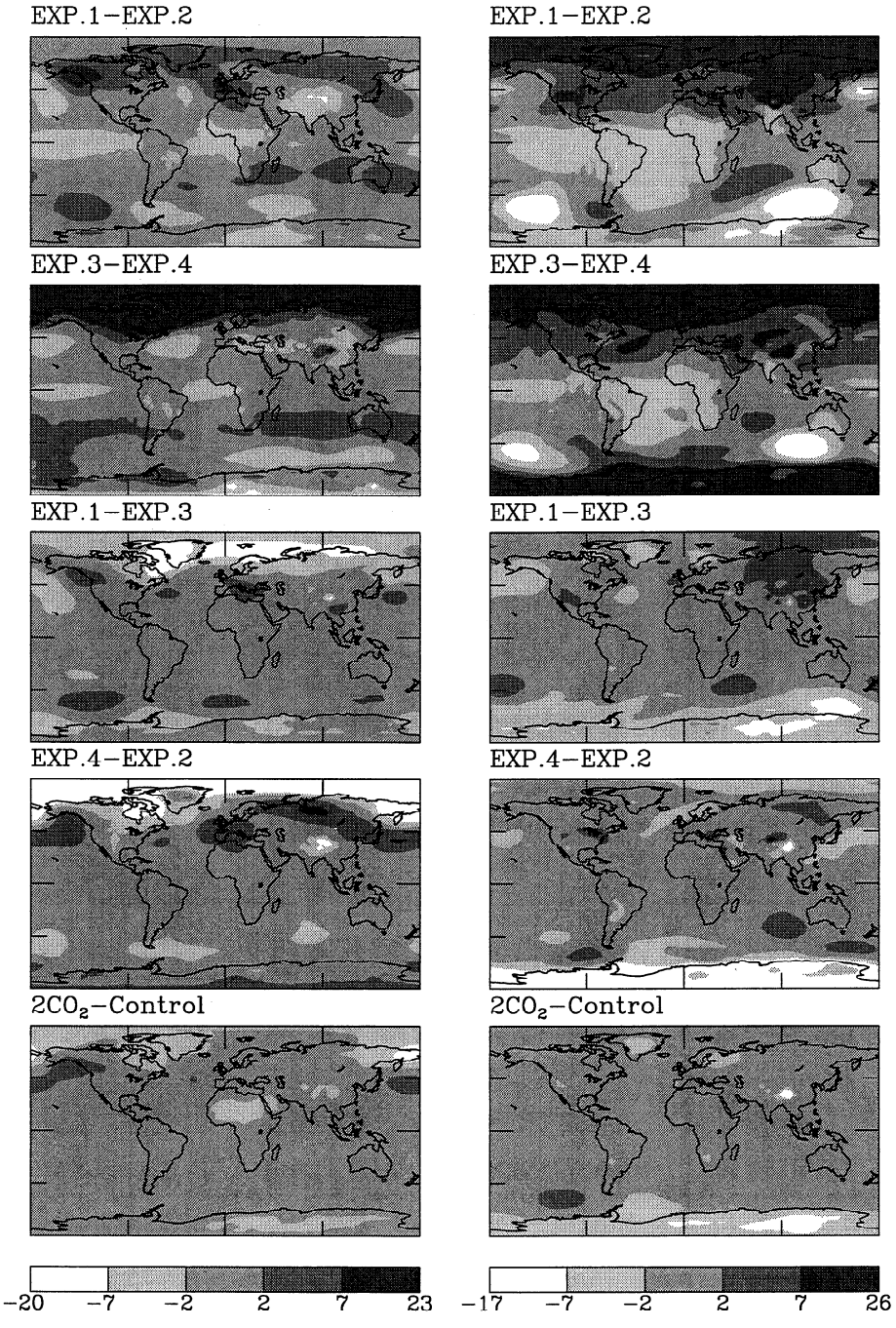

Figure 9. As in Plate 2 except for sea level pressure (mbar).

occurs around the lows near Antarctica. Most of these effects are more obvious during winter.

The location of the synoptic changes is related to changes in planetary wavenumbers 3–5. The 500 mbar height variations are given in Figure 11. The mean atmospheric troughs over the North Pacific, western Atlantic, and central Europe all deepen somewhat in their current position, while the warmer tropics and subtropics experience increased ridging. The effect over the North Pacific is much stronger than that over the North Atlantic, which is then reflected in the sea level pressure field. The mean troughs also deepen around Antarctica.

The planetary wave changes and the latitudinal temperature increase result in the 200 mbar (jet stream) wind changes shown in Figure 12. Intensified subtropical jets appear with the increased gradient. Storms will follow these wind changes and therefore would be expected to be preferentially directed in winter, for example, along the southern border of the United States as well as northward toward Alaska and along the east coast of Asia to Japan.

The precipitation changes, resulting from mean circulation and eddy influences, show that with the increased gradient, tropical precipitation increases primarily over the oceans, while there are general decreases over most subtropical areas (Plate 3). The monsoon over India weakens, and northern Australia has less precipitation in summer, consistent with the reduction in the summer hemisphere Hadley circulation upwelling due to equatorial latent heat forcing. Extratropical winter precipitation patterns are generally consistent with

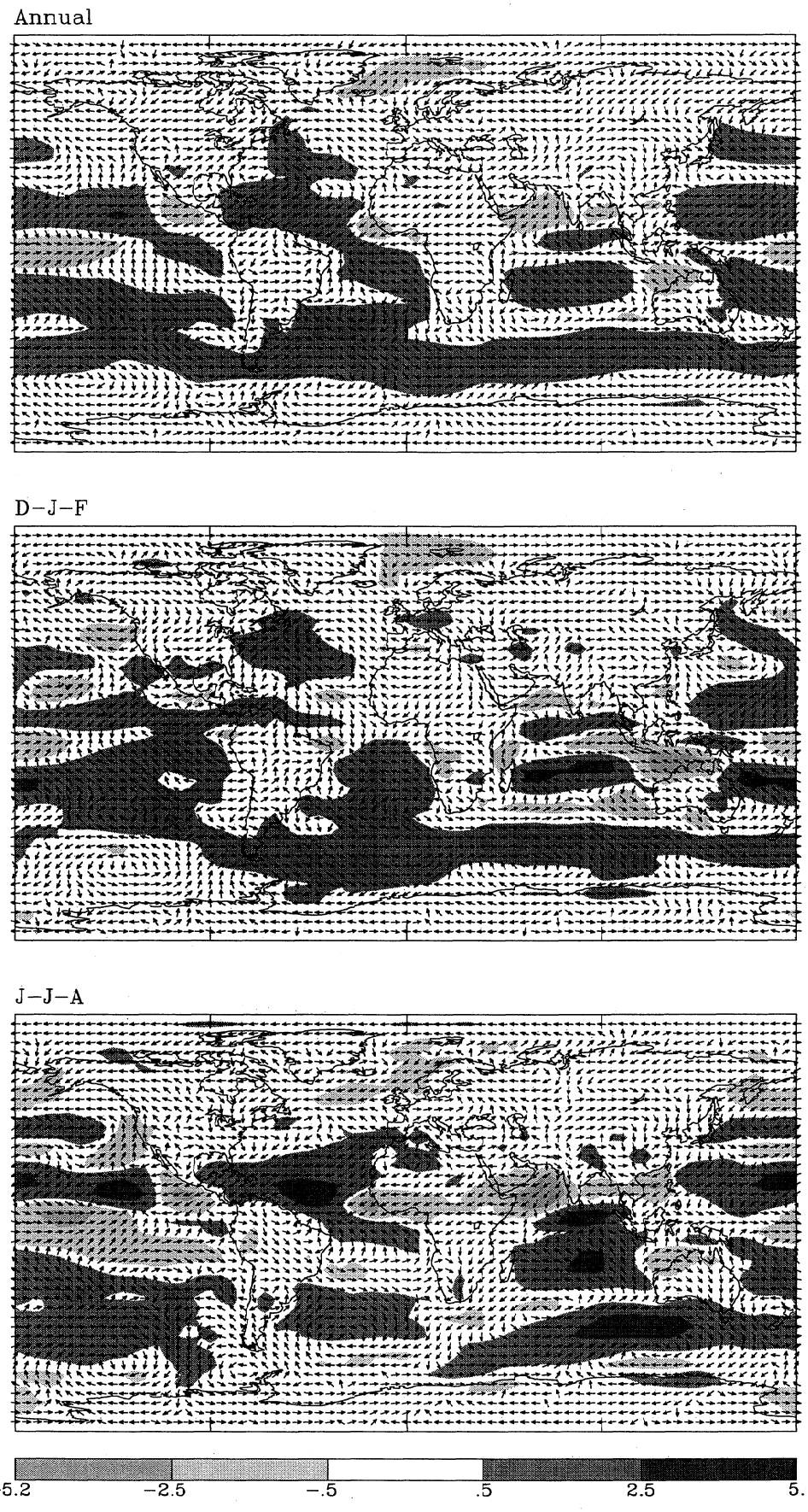

Figure 10. Change in surface winds between experiments 1 and 2 for the annual average and two solstice seasons. Arrows indicate direction, shading indicates magnitude (i.e., negative values indicate weakening of total magnitude). Units m s^{-1}.

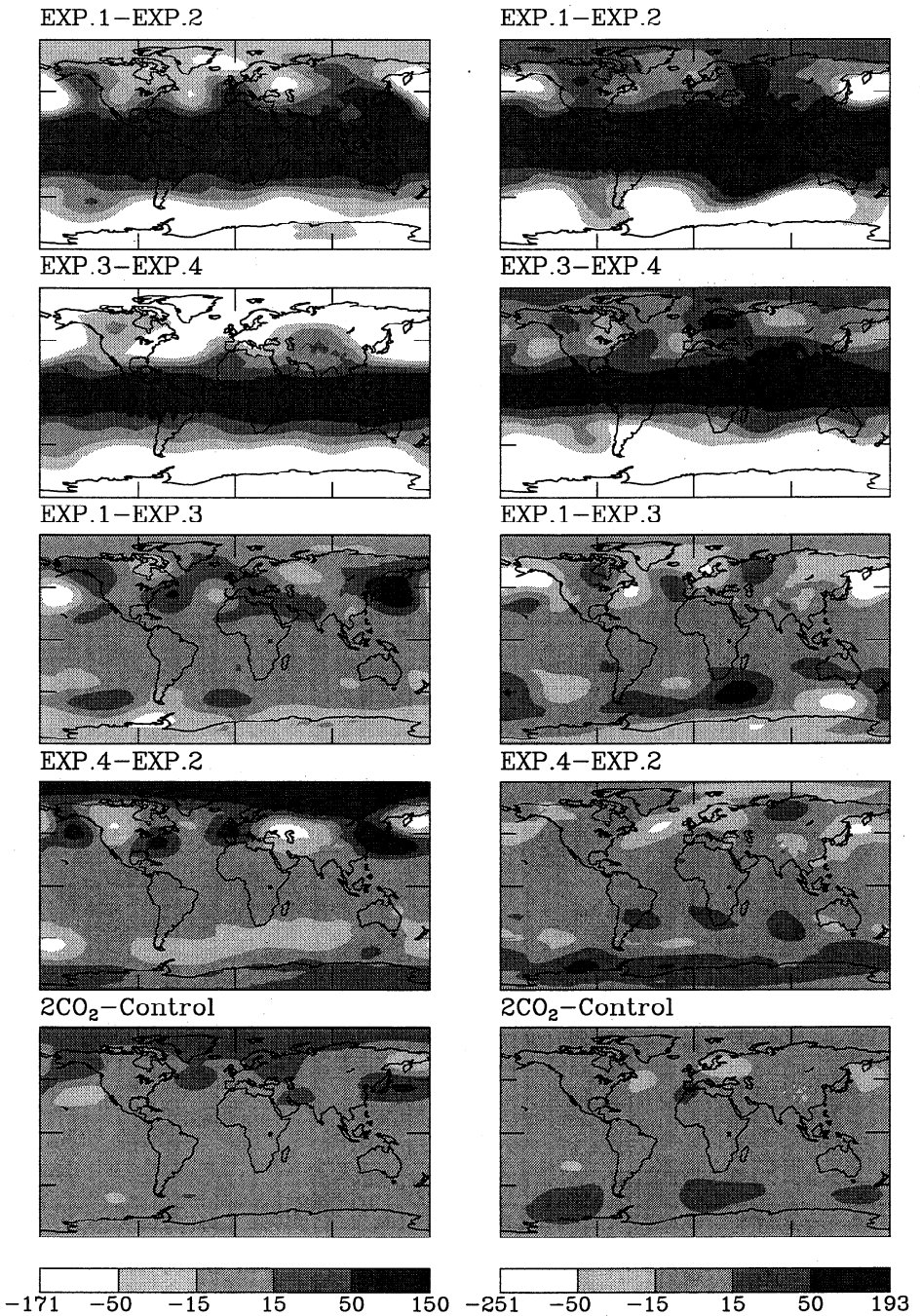

Figure 11. As in Plate 2 except for 500 mbar heights (m). To make the scales commensurate, the following values have been added to each point in the figure: 176.7 m (row 2), −102.7 m (row 3), −106.8 m (row 4) and −72.5 m (row 5).

storm track changes, as estimated from the jet stream response described above.

The soil moisture changes show general drying in the subtropics (Plate 4). A narrow band of moistening occurs over some tropical land areas. In general, wetter conditions prevail for the central and eastern United States. The soil moisture changes generally follow the precipitation changes, with modification due to the increased evaporation with warmer temperatures.

The results for experiment 1 minus experiment 2 in specific regions of interest are presented in Table 4, along with the interannual standard deviations (in parentheses). As expected, middle- and high-latitude regions cool, and low and subtropical regions warm. Over the United States, in general, there are increases in precipitation, soil moisture, runoff, snow cover, and cloud cover. In Eurasia, while precipitation itself is slightly reduced, more of it falls as snow, and there is less melting, so snow cover still increases. Subtropical areas have less precipitation due to increased subsidence over most longitudes; since the warmer temperatures also lead to an increase in evaporation, these areas are drier with reduced runoff and reduced cloud cover.

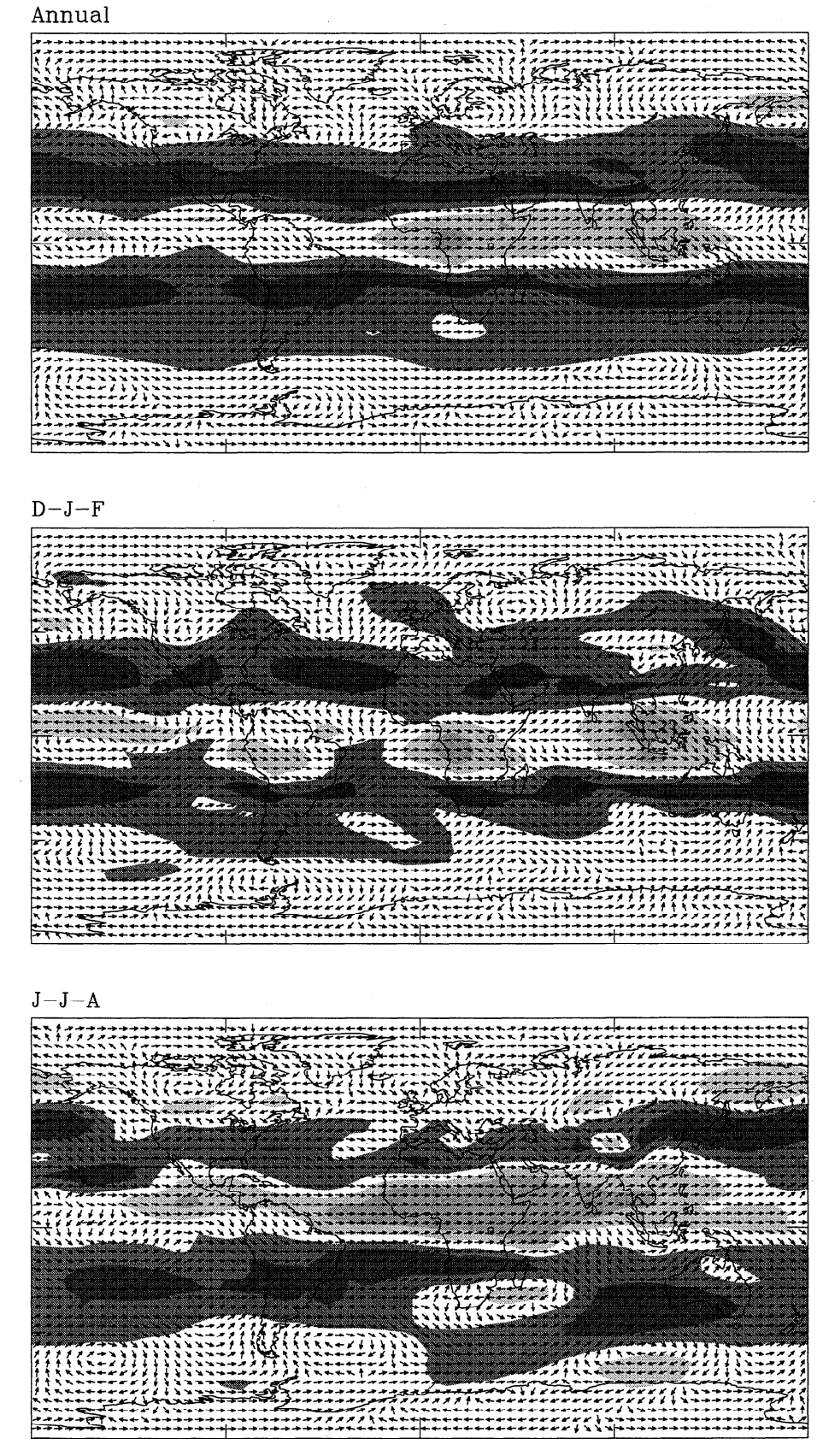

Figure 12. As in Figure 10 except for 200 mbar winds (m s ^{1}).

Even in some tropical locations, experiment 1 is drier than experiment 2, which indicates that with cooler tropical sea surface temperatures the land can be wetter (Table 4 and Plate 4). Apparently, the effects of the change in land/ocean circulation patterns, which dry the tropical land areas in experiment 1, can be comparable to the influence of the reduced moisture availability in experiment 2. Therefore changes in tropical soil moisture or lake levels are not so useful an indicator of low-latitude temperature gradients as are observed changes in subtropical moisture.

Considering the ice core regions, in Greenland with the increased gradient the temperature cools, with little change in the annual hydrologic cycle. In southern China, near the Tibetan Plateau, the temperature warms, and it is somewhat wetter. In Peru from 8° to 12°S conditions are warmer, and it is somewhat drier, especially in summer. Over Antarctica the temperature is again cooler, with the Vostok ice core region showing some moderation during summer due to advective influences from the stronger offshore lows; overall, there is slightly reduced precipitation. Not shown in the table, snow depth decreases slightly over Greenland, with little change over Antarctica.

4. Results of Altering the Latitudinal Temperature Gradient With a Global Temperature Change

How are the conclusions derived above for the effect of gradient changes altered when the global climate itself is allowed to change? For this we make comparisons to the conclusions given above using experiment 3, in which the increased gradient was accompanied by colder global temperatures, and experiment 4, in which the decreased gradient was accompanied by warmer global temperatures.

The surface air temperature differences between these experiments and the control run are shown in Figure 1. From 60°N to 60°S the gradient changes are similar to those in experiments 1 and 2, with the mean temperatures offset. At the highest latitudes during winter, due to the sea ice changes, experiment 3 has a strong increase in gradient, while experiment 4 has a strong decrease.

The differences between each experiment and control are given in the figures and tables already presented, with regional changes shown in Table 5. The global average results (Table 1) show that the surface air temperatures between the experiments differ by close to 10°C and the air temperatures by 9°C. In the tropics the temperatures in the two experiments differ by 3°C near the surface and 6°C near the tropopause; at high latitudes they differ by more than 20°C at low levels, with only small changes in the upper troposphere. The pattern of the differences are therefore similar to those shown in Plate 1, only more extreme. The lapse rate in experiment 4 is increased because of the high-latitude changes, although in the tropics, the total lapse rate and the moist adiabatic value are less due to the added moisture.

Comparison of the four experiments in Table 1 allows us to determine what aspects of the global climate change, associated with a change in the latitudinal temperature gradient, would remain if, in addition, the global mean temperature itself changed. With an increased gradient (experiment 1) the globe had more rainfall, more atmospheric water vapor, more cloud liquid water, higher ground and planetary albedos, and a reduced lapse rate. When this increased gradient is associated with a colder climate globally (experiment 3), and particularly in the tropics, there is less rainfall, less water vapor, less cloud liquid water; only the higher ground and planetary albedos and the reduced lapse rate remain. The difference primarily relates to the tropical sea surface temperatures, which are warmer than in the control run in experiment 1, and colder than the control run in experiment 3. High latitudes are cooler in both experiments. Experiments 2 and 4 produce similar differences for the same reasons: experiment 2 had cooler tropical temperatures than the control, while they are now warmer in experiment 4; both are warmer at high latitudes. In addition, since experiment 4 has greatly reduced sea ice at high latitudes, the low-level air temperatures are much warmer, and low cloud cover is greater.

The hydrologic cycle and low-latitude circulation changes are given in Figures 2–5 and Table 2. In almost all respects the latitudinal patterns of change closely mimic those from experiments 1 and 2. This result indicates that the distribution of rainfall and associated dynamics is determined primarily by the latitudinal gradient and not by the mean global temperature. This is in contrast to the global average results which depended primarily on the magnitude of the global mean temperature.

Energy results are presented in Figure 6 and Table 3. As was the case for the latitudinal expression of the hydrologic cycle, eddy processes are dominated by the latitudinal temperature gradient, and the global climate change does little to alter the main effects: experiments 3 and 1 are very similar in their response, as are experiments 4 and 2. Minor differences exist: the gain in EAPE in experiment 2 from the warm high-latitude sea surface temperatures does not occur in experiment 4, presumably because the air is now so warm that the land has warmed as well. Hence there is a greater decrease in $P \rightarrow K$, and changes in EKE are now antisymmetric. The radiative damping of EAPE is also somewhat reduced, responding to the decreased EAPE. Nevertheless, the midlatitude energy cycle, like the low-latitude Hadley circulation, responds to the temperature gradient much more than the absolute value of the temperatures. The biggest change between experiments 3 and 4 again occurs for wavenumbers 3–8 (Figure 6), antisymmetrical this time. Despite the much larger changes in the high-latitude gradient the results from experiments 3 and 4, shown in Table 3 and Figure 6, look much like those from experiments 1 and 2; the gradient changes in the sea ice zones apparently do not impact hemispheric average eddy processes significantly. The ratio of standing to transient eddy energy again shows only little variation, averaging 12.2% on the annual average in experiment 3 and 13.8% in experiment 4. The slight reduction in experiment 3 may be due to a reduced land/ocean temperature gradient with more sea ice.

The energy transport changes generally mimic those that occurred in experiments 1 and 2, although the global temperature does affect the ambient water vapor levels and latent heat transports. Comparing experiments 1 and 3, dry static energy transports are similar, but latent heat transport decreases in the colder experiment (experiment 3) by 20%. Therefore total atmospheric transports are 7% less. Comparing experiments 2 and 4, dry static energy transport drops slightly in the warm experiment (experiment 4), but latent heat transport increases by 30%. Therefore total atmospheric transports increase by about 10%.

The various regional changes between experiments 3 and 4 are given in Table 5 and Plate 2, Figures 9 and 11, and Plates 3 and 4. Much larger temperature differences now exist (Plate

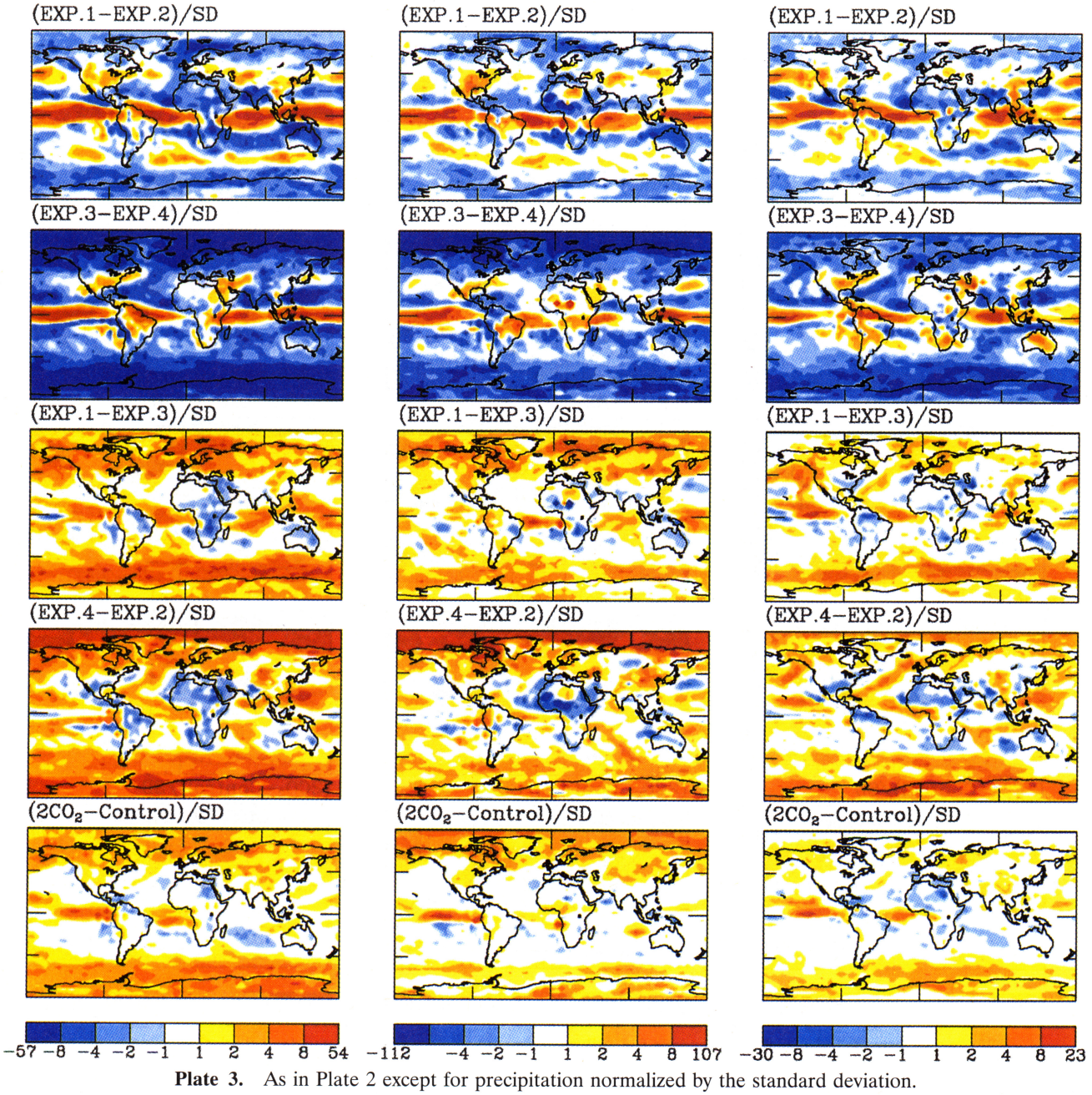

Plate 3. As in Plate 2 except for precipitation normalized by the standard deviation.

2), and the increase of sea level pressure at high latitudes is somewhat greater (Figure 9). However, as would be implied by the similar eddy and Hadley cell changes, most of the sea level pressure and 500 mbar differences generated by the increased gradient are still apparent. The high-latitude differences in precipitation are more exaggerated (Plate 3), and the tropics are more clearly wetter (Plate 4), while the subtropical drying is somewhat reduced, due to the overall decrease in temperature-driven evaporation.

5. Results of Altering the Global Mean Temperature With Little Temperature Gradient Change

Comparisons of experiments 1 and 3, and 2 and 4, allow us to investigate what happens when the global mean temperature is altered without a temperature gradient change, at least from 60°N to 60°S. Global average results presented in the previous section indicated that global properties are dominated by the tropical temperature change, which also affects energy transports, particularly the transport of latent heat. Experiment 1 is warmer than experiment 3 at all latitudes (Figure 1), which is also true for experiment 4 compared with experiment 2; in both cases the global mean temperature difference is about 5°C. The difference between them is the experiments 1 and 3 combination occurs in runs whose average temperature is at or below control run values and with an increase in latitudinal temperature gradient relative to the control run, while the opposite applies for the experiments 2 and 4 combination.

In both sets of experiments the warmer run has less low cloud cover, more high cloud cover and cloud liquid water,

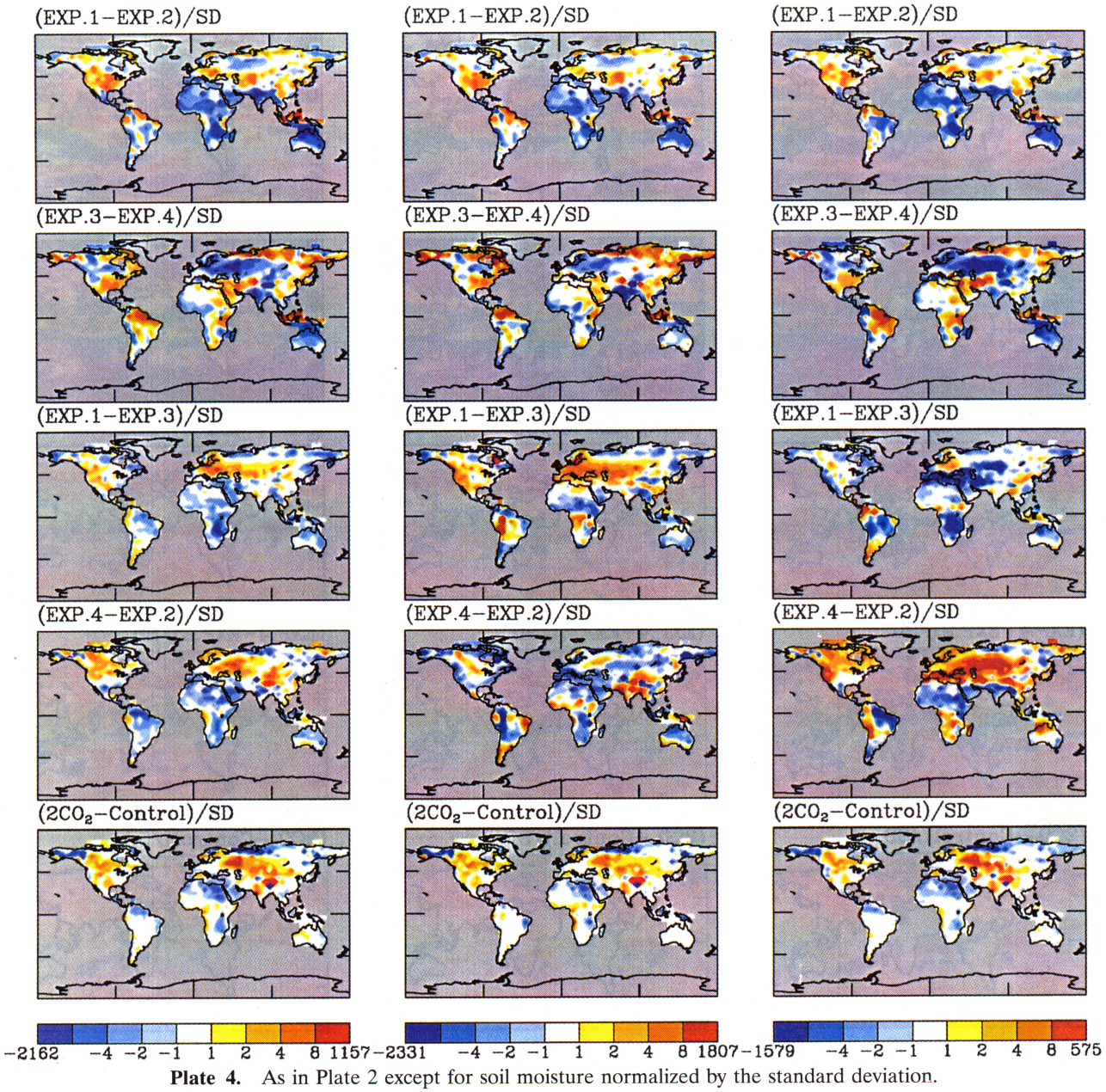

Plate 4. As in Plate 2 except for soil moisture normalized by the standard deviation.

more precipitation at all latitudes (zonally averaged), but less precipitation and soil moisture over land from 30°N to 30°S, and more from 30° to 60°N (Figures 2–5). The tropical precipitation over land is affected by the land/ocean contrast, and when the oceans are warmer, there is more subsidence over land. The Hadley cell is generally somewhat weaker with a poleward expansion of extent in the warmer run. Eddy kinetic energy is somewhat weaker (Table 3); however, the polar lows are affected by the latitudinal temperature gradient change which does exist poleward of 60° latitude: the big decrease in wintertime gradient weakens the Aleutian low in experiment 4, but the presence of substantial sea ice appears to weaken this low in experiment 3, hence producing opposite effects in the two sets of simulations (Figure 9). In contrast, the northeastern portion of the Icelandic low is somewhat deeper in each of the warmer runs, being farther poleward than then Aleutian low, in a region where high pressure dominates in the colder experiments. This latter effect also applies in the southern hemisphere, where the Subantarctic lows are deeper in the warmer runs.

The absolute magnitude of the temperatures do appear to have some effect on the regional hydrologic differences. Experiments 4 minus 2 show greater low/subtropical latitude precipitation reduction over some land areas (Plate 3). While the temperature differences are similar in the two sets of experiments, the water vapor holding capacity, following the Clausius-Clapeyron relation, is not and is greater in experiments 4 minus 2 (e.g., Table 1 for atmospheric water vapor). The warm ocean/cooler land contrast can thus lead to more intensified longitudinal cells, with greater subsidence over land. Some differences in soil moisture at these latitudes then also arise (Plate 4).

6. Results From Different Climate Forcing

Finally, the results presented so far arose from a change in gradient due to a specific mechanism of change, i.e., an implicit change in ocean heat transports, or global climate change due to specification of different sea surface temperatures. Would

Table 4. Change in Annual Climate Parameters, Experiment 1 Minus Experiment 2

	Temp., °C	Precip., mm d^{-1}	Soil Moisture, mm	Runoff, mm d^{-1}	Snow Cover, %	Cloud Cover, %
West United States	−2.4 (0.07)	0.5 (0.16)	46 (13)	0.3 (0.07)	8.1 (2.4)	9 (1.9)
Central United States	−2.3 (0.07)	1.2 (0.36)	214 (39)	0.7 (0.17)	5.7 (1.4)	9 (3.2)
East United States	−1.1 (0.05)	0.7 (0.3)	34 (18)	0.5 (0.15)	3.8 (1.9)	2 (2.4)
South Canada	−3.0 (0.08)	0.0 (0.1)	−28 (28)	0.2 (0.05)	9.1 (2.4)	2 (1.4)
Greenland	−3.2 (0.05)	−0.3 (0.12)	0.0 (0)	−0.1 (0.02)	0.2 (0.15)	0 (0.8)
Mid-Europe	−3.1 (0.04)	0.0 (0.2)	32 (15)	0.0 (0.07	5.0 (1.4)	1 (2.1)
North Russia	−2.1 (0.06)	−0.3 (0.22)	−66 (47)	0.2 (0.09)	10.1 (2.7)	−2 (3.3)
West Siberia	−2.8 (0.07)	−0.5 (0.14)	−22 (8)	0.0 (0.06)	4.8 (2.1)	−5 (2.4)
Siberian Plateau	−3.3 (0.04)	−0.3 (0.1)	−2 (3)	0.0 (0.08)	3.3 (1.3)	−2 (1.6)
South China	0.8 (0.05)	1.1 (0.48)	47 (21)	0.8 (0.29)	−2.5 (1.0)	2 (2.5)
China Desert	0.4 (0.05	0.0 (0.26)	−10 (17)	0.0 (0.12)	−2.2 (1.9)	−1 (2.9)
Indian Desert	6.7 (0.05)	−2.7 (0.23)	−87 (7)	−1.8 (0.19)	−1.7 (0.5)	−17 (1.8)
Australian Desert	4.5 (0.04)	−1.5 (0.32)	−95 (12)	−0.6 (0.1)	0 (0)	−19 (4.4)
North Sahara	1.1 (0.05)	−0.2 (0.12)	−20 (9)	−0.1 (0.04)	0 (0)	−4 (3.4)
South Sahara	4.8 (0.03	−1.6 (0.36)	−67 (12)	−0.5 (0.12)	0 (0)	−14 (4.3)
African Sahel	7.7 (0.05)	−1.6 (0.45)	−154 (22)	−1.0 (0.19)	0 (0)	−20 (4.0)
African rain forest	5.9 (0.02)	−0.6 (0.31)	−86 (19)	−0.3 (0.15)	0 (0)	−6 (1.7)
Amazon rain forest	5.6 (0.02)	0.1 (0.24)	−33 (14)	0.4 (0.14)	0 (0)	−6 (1.6)
Antarctica	−4.2 (0.03)	−0.1 (0.02)	0 (0)	0 (0.00)	0 (0)	−1.5 (0.6)

Standard deviations are shown in parentheses.

the changes in gradient/temperature arising from a different mechanism produce similar responses? To investigate this question, we use a control and doubled CO_2 experiment run with a "q-flux" mixed layer ocean, hence an ocean in which heat transports are not allowed to be changed. We then see whether the expectations generated in the previous section are consistent with the changed gradient and temperature from this entirely different forcing.

In the doubled CO_2 experiment, surface air temperature is warmed by 3.5°C. The warming as a function of latitude is shown in Figure 13 (top). While the warming is greater at high latitudes on the annual average, there is actually little temperature gradient change between the equator and 50°S, and even in the northern hemisphere the change is muted between the equator and 40°N compared to the differences given in Figure 1. In this respect the doubled CO_2 climate simulation simply has warmer temperatures, similar to the differences discussed in the previous section between experiments 1 and 3, and 2 and 4, which are shown for comparison.

While a complete analysis of the reasons for the doubled CO_2 result is beyond the scope of this paper and is, in fact, being given elsewhere [*Tselioudis et al.*, 1997], the magnitude of the tropical warming and the lack of substantial gradient change through midlatitudes is a result of both the model's penetrative convection scheme and its cloud liquid water budget parameterization. Similar to observations for today's climate [*Tselioudis et al.*, 1992], the model reduces its cloud optical thickness at lower latitudes as climate warms, hence amplifying the cloud feedback at these latitudes. At higher latitudes the additional moisture leads to thicker clouds, a negative feedback for global warming. The net effect is to produce a small change in gradient of surface warming. Whether this is an accurate indication of what the doubled CO_2 equilibrium climate would really be like is open to debate; for our purposes, however, its use is primarily to investigate whether the expectations generated from experiments 1 to 4 are consistent with the results from a completely different forcing.

Table 5. Change in Annual Climate Parameters, Experiment 3 minus Experiment 4

	Temp., °C	Precip., mm d^{-1}	Soil Moisture, mm	Runoff, mm d^{-1}	Snow Cover, %	Cloud Cover, %
West United States	−11.7 (0.07)	−0.2 (0.16)	−11.8 (13)	0 (0.07)	30 (2.4)	4 (1.9)
Central United States	−13.5 (0.07)	0.5 (0.36)	157 (39)	0.5 (0.17)	18 (1.4)	8 (3.2)
East United States	−12.9 (0.05)	0.4 (0.3)	82.3 (18)	0.6 (0.15)	25 (1.9)	5 (2.4)
South Canada	−12.5 (0.08)	−1.3 (0.1)	−72 (28)	1.1 (0.05)	33.3 (2.4)	−10 (1.4)
Greenland	−17.6 (0.05)	−1.5 (0.12)	39.8 (0)	−0.7 (0.02)	6.7 (0.15)	−10 (0.8)
Mid-Europe	−12.9 (0.04)	−1.2 (0.2)	−73 (15)	−0.2 (0.07)	28.2 (1.4)	−6 (2.1)
North Russia	−12.4 (0.06)	−1.6 (0.22)	−187 (47)	−0.3 (0.09)	30.3 (2.7)	−17 (3.3)
West Siberia	−14.4 (0.07)	−1.2 (0.14)	16 (8)	−0.3 (0.06)	23.3 (2.1)	−10 (2.4)
Siberian Plateau	−16.0 (0.04)	−1.0 (0.1)	40 (3)	−0.3 (0.08)	19.6 (1.3)	−10 (1.6)
South China	7.2 (0.05)	−.5 (0.48)	14.6 (21)	−0.4 (0.29)	8.3 (1.0)	1 (2.5)
China Desert	9.1 (0.05)	−1.0 (0.26)	−28 (17)	−0.4 (0.12)	17.5 (1.9)	−12 (2.9)
Indian Desert	7.1 (0.05)	−0.9 (0.23)	−45 (7)	−1.1 (0.19)	5.9 (0.5)	−6 (1.8)
Australian Desert	7.4 (0.04)	0 (0.32)	−48.3 (12)	−0.4 (0.1)	0.3 (0)	−8 (4.4)
North Sahara	9.3 (0.05)	−0.2 (0.12)	1.4 (9)	0.1 (0.04)	0.3 (0)	4 (3.4)
South Sahara	7.9 (0.03)	−0.2 (0.36)	−3.6 (12)	0 (0.12)	0 (0)	−0 (4.3)
African Sahel	5.7 (0.05)	−0.7 (0.45)	−34 (22)	−0.3 (0.19)	0 (0)	−4 (4.0)
African rain forest	5.1 (0.02)	1.0 (3.1)	39.8 (19)	0.5 (0.15)	0 (0)	3 (1.7)
Amazon rain forest	6.0 (0.02)	1.6 (0.24)	75 (14)	1.4 (0.14)	0 (0)	10 (1.6)
Antarctica	−20.1 (0.03)	−0.7 (0.02)	0 (0)	−0.45 (0.00)	6.5 (0)	−1 (0.6)

Table 6. Change in Annual Climate Parameters, $2CO_2$ Minus Control

	Temp., °C	Precip., mm d^{-1}	Soil Moisture, mm	Runoff, mm d^{-1}	Snow Cover, %	Cloud Cover, %
West United States	4.24 (0.07)	0.3 (0.16)	27.1 (13)	0.01 (0.07)	−15.6 (2.4)	2.7 (1.9)
Central United States	3.62 (0.07)	0.6 (0.36)	46.8 (39)	0.3 (0.17)	−7.3 (1.4)	3.6 (3.2)
East United States	3.81 (0.05)	0.3 (0.3)	1.6 (18)	0.1 (0.15)	−9.4 (1.9)	0.8 (2.4)
South Canada	3.33 (0.08)	0.4 (0.1)	126.1 (28)	−0.1 (0.05)	−6.7 (2.4)	2.3 (1.4)
Greenland	5.81 (0.05)	0.5 (0.12)	−9.5 (0)	0.2 (0.02)	−1.4 (0.15)	2 (0.8)
Mid-Europe	3.30 (0.04)	0.2 (0.2)	−11.1 (15)	0.1 (0.07)	−8.9 (1.4)	0 (2.1)
North Russia	3.71 (0.06)	0.6 (0.22)	154.5 (47)	−0.1 (0.09)	−8.1 (2.7)	4.3 (3.3)
West Siberia	4.18 (0.07)	0.4 (0.14)	−24.5 (8)	0.2 (0.06)	−5.1 (2.1)	2.2 (2.4)
Siberian Plateau	4.32 (0.04)	0.3 (0.1)	−14.3 (3)	0.2 (0.08)	−5.2 (1.3)	1 (1.6)
South China	3.96 (0.05)	0.4 (0.48)	−15.5 (21)	0 (0.29)	−6.2 (1.0)	−0 (2.5)
China Desert	3.88 (0.05)	0.5 (0.26)	46.7 (17)	0.2 (0.12)	−9.1 (1.9)	−5.5 (2.9)
Indian Desert	4.44 (0.05)	0.1 (0.23)	8.5 (7)	0.1 (0.19)	−3.3 (0.5)	1.2 (1.8)
Australian Desert	4.05 (0.04)	0.1 (0.32)	11.1 (12)	0.1 (0.1)	0 (0)	0 (4.4)
North Sahara	4.64 (0.05)	−0.1 (0.12)	−12.0 (9)	−0.0 (0.04)	0 (0)	−2.1 (3.4)
South Sahara	5.52 (0.03)	−0.3 (0.36)	−26.5 (12)	−0.1 (0.12)	0 (0)	−2 (4.3)
African Sahel	4.91 (0.05)	−0.1 (0.45)	−4.0 (22)	−0.0 (0.19)	0 (0)	1.3 (4.0)
African rain forest	3.73 (0.02)	0.1 (0.31)	−11.9 (19)	0.1 (0.15)	0 (0)	0.4 (1.7)
Amazon rain forest	3.65 (0.02)	−0.2 (0.24)	−19.5 (14)	0.1 (0.14)	0 (0)	−3.4 (1.6)
Antarctica	5.33 (0.03)	0.1 (0.02)	0 (0)	0.1 (0.00)	−1.0 (0)	2.4 (0.6)

The results from this experiment are given in Tables 1–3, Table 6, and Plate 2, Figures 9 and 11, and Plates 3 and 4. Based on the analysis of a "simply warmer" experiment with little gradient change, the doubled CO_2 climate (relative to its control) fulfills all the expectations presented in the previous sections: more high cloud cover and cloud liquid water, more precipitation, but less precipitation and soil moisture over land from 30°N to 30°S, with more from 30° to 60°N. The most notable difference is that the hydrologic cycle changes (precipitation changes, drying at low latitudes) are weaker; not only is the low-latitude warming weaker (Figure 13), but so is the contrast between land and ocean warming. For example, the ocean/land surface temperature warming in winter at 30°–60°N in experiment 2 was 1.5°C/0.9°C, in experiment 4 it was 6.2°C/5.5°C, and in the $2 \times CO_2$ experiment it was 2.8/3.1°C. Since increased CO_2 is directly heating the land as well as the ocean, the subsidence experienced over tropical land from the ocean transport experiments is diminished, and the drying is less.

Another change which occurs because of this land/ocean differential is that there is less condensational production of eddy available potential energy. Since in winter condensational heat release occurs preferentially over the oceans, heat is now being added to the region which is relatively cooler, reducing EAPE generation. Overall, EAPE changes follow the land/ocean heating differential, being positive in experiment 2, showing little change in experiment 4, and decreasing with doubled CO_2. The importance of this result is that mechanisms which heat the high-latitude ocean directly, such as ocean heat transport increases, suffer less decrease in baroclinic production (experiment 2) with a latitudinal temperature gradient reduction than do climate forcings that warm the land preferentially (doubled CO_2).

The land/ocean warming differential affects an additional feature of the simulation: while there are still substantial energy decreases in wave 3, and waves 3–8, in general, during northern hemisphere winter, now wave 1 also experiences strong reduction. Therefore although the Aleutian low still decreases (Figure 9), the Icelandic low is less affected. Apparently, preferential warming over the ocean in the previous experiments 2 and 4 helped maintain wave 1 energy even with the latitudinal temperature gradient reduction, by maintaining a strong land/ocean contrast. Nevertheless, once again the ratio of stationary to transient eddy energy is unaffected by the climate change, being 11.5% in the doubled CO_2 control run and 11.8% in the doubled CO_2 experiment.

Considering the regional changes, the doubled CO_2 experiment maintains many of the overall characteristics of the "warm-cool" experiments (Plates 3 and 4) with the principal exception that the changes from 30°N to 30°S are more muted. The distinctions which do occur may allow CO_2 forcing to be distinguished from ocean heat transport changes in the paleorecord.

7. Discussion

The preceding experiments have indicated what might be expected, from the GCM used, when the latitudinal temperature gradient changes without a global mean temperature change, when the gradient change is accompanied by global temperature changes, and when the mean global temperature changes without a change in gradient for most of the planet. Results for both an (implicit) change in ocean heat transport and a change in atmospheric CO_2 produce generally similar effects. Since both ocean heat transport and CO_2 changes are leading potential causes for paleoclimate variations, understandings arrived at in the previous sections should be relevant for paleoclimate considerations. However, there are some forcings, such as orbital variations, that likely will produce different latitudinal and seasonal patterns not derivable from these experiments.

With the foregoing results, we can now investigate paleoclimate evidence in an attempt to deduce what happened to the latitudinal temperature gradient in paleoclimates, what might be expected for future anthropogenic warming, and the relevance of ice core results to global climate changes.

For the paleoclimate comparison the procedure is as follows: we first review available evidence of temperature reconstructions of the latitudinal gradient for each time period and then evidence for the moisture distributions. We use the previous experiments to see if the two sources of evidence are consistent. An additional source of paleoclimatic data, eolian data (grain size and mass flux) which provide information

about aridity and wind speeds are available for further consistency checks. It must be emphasized that paleodata may have more than one interpretation, probably more true the farther back in time one looks, so the following discussion is of necessity speculative in nature.

7.1. Paleolatitudinal Temperature Gradients

Most of the discussion concerns the northern hemisphere, where more paleodata are available. In some cases, variations need to be ignored within the broad-scale climate eras to focus on general conditions.

7.1.1. Mesozoic climates. Admittedly, the data available for reconstructing these climates are less precise than for later time periods. Nevertheless, from oxygen isotope, biogeographic, and lithologic information, *Frakes* [1979] and *Horrell* [1990] infer significant warming (10°C or more) at high latitudes in the Mesozoic. At low latitudes, oxygen isotope data suggest there was little change, leading *Frakes* [1979] to conclude that the latitudinal temperature gradient may have been reduced by a factor of 2. Do the results of the experiments discussed here support this assessment? (An additional caveat appropriate here is that the model experiments were conducted with the present continental distribution, which does make them somewhat less relevant for this time period).

Reconstructions based on soil types suggest that the Mesozoic climate featured aridity in the tropics and subtropics during the Triassic and Jurassic and moist conditions at high latitudes [*Parish et al.*, 1982; *Hallam*, 1985; *Ronov et al.*, 1989]. Some of this aridity may have been the result of the large single continent that existed during part of this period, but the aridity was apparently maintained after the continental breakup. These results are not consistent with the reduced temperature gradients in experiment 2 but look more like the results from a warm climate with little gradient change (Figure 13, bottom). A reduction in the latitudinal temperature gradient, as implied by tropical isotopic evidence, would have produced a reduction in Hadley cell intensity and hence wetter conditions in the subtropics (Figure 5), apparently inconsistent with the data. *Hay et al.* [1990] note that the existence of a tropical continent would have had the effect of maintaining a large latitudinal temperature gradient (in effect, adding another latitude-dependent forcing), but this cannot be the primary explanation, for when the continents broke up, the very warm tropical continent would have had enough moisture to produce monsoons and a tropical rainbelt, which apparently did not occur [*Frakes et al.*, 1992]. *Pollard and Schulz* [1994] suggested small-scale orography could have played a role, while *Rind et al.* [1990] suggested that aridity would arise when the tropics were significantly warmer than today, as the air would be able to hold more moisture, amplifying evaporation. In the GCM experiments, a 5°C tropical warming, while maintaining current temperature gradients, was sufficient to produce drier conditions from 30°N to 30°S (Figure 13, bottom).

The assumption of a very warm tropics during this period requires dismissal of the ocean isotope evidence. *Horrell* [1990] argues that such dismissal is warranted because it implies an actual reversal of the latitudinal temperature gradient: terrestrial floral evidence for southeastern North America indicates temperatures far exceeding isotope-derived tropical temperatures, while high-latitude isotope-derived sea surface temperatures (above 60° paleolatitude) give warmer values than indicated for the tropics. However, while the marine isotopic record does require assumptions about global ice volume and

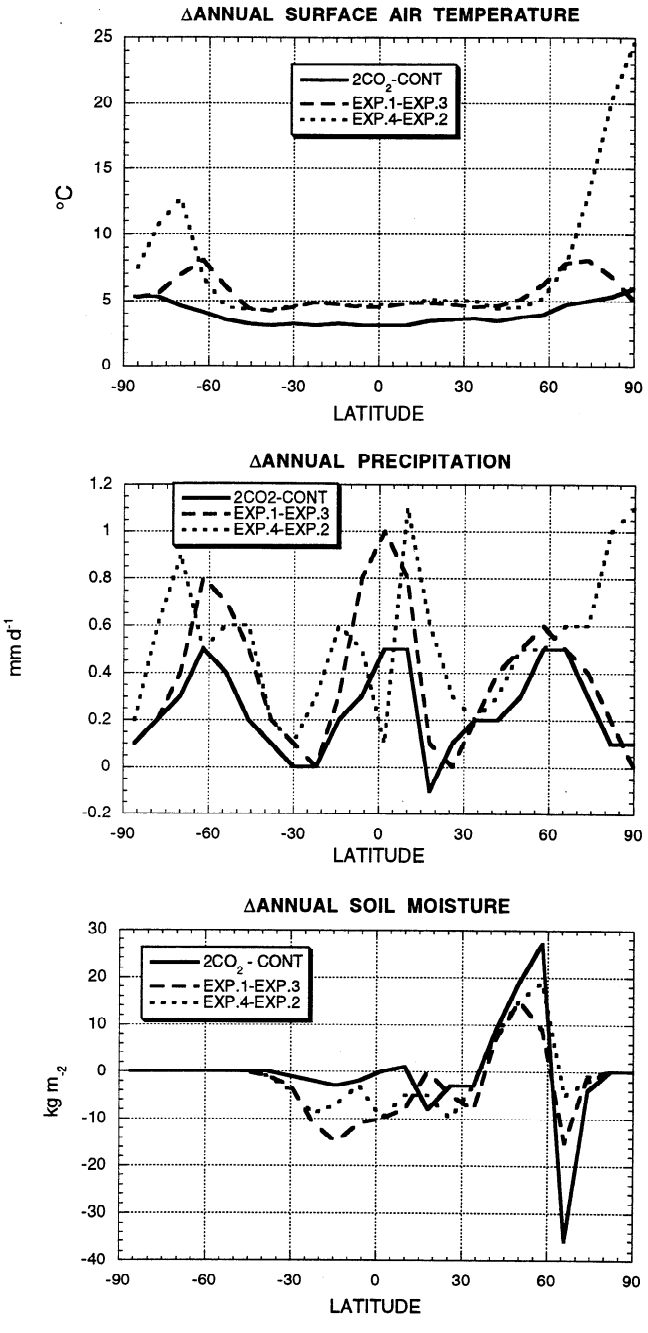

Figure 13. Change in annual surface air temperature (top), precipitation (middle), and soil moisture (bottom) for the doubled CO_2 experiment and for experiments 1 minus 3 and 4 minus 2.

local salinity, it is unsatisfactory to simply assume it is wrong; hence understanding of the consistency of the temperature and moisture fields is of paramount importance to understanding the climate of this era. If isotope work based on biogenic phosphates and chert-phosphate pairs is accepted, subtropical sea surface temperatures may have been as high as 38°C [*Frakes et al.*, 1992].

The extratropical temperature gradient was less than at present for much of this era, especially without the existence of land ice, as shown, for example, in the early Jurassic simulation of *Chandler et al.* [1994]. This results suggests that the tropical and extratropical latitudinal temperature gradients may

change in different ways as climate changes. Very warm conditions at high latitudes are consistent with the formulation in experiment 4 and would therefore suggest that the extratropical regions would have reduced eddy energy, shorter atmospheric waves, and greater precipitation at the highest latitudes. With warm conditions prevailing at both low and high latitudes, cloud optical thickness would have been larger, increasing atmospheric albedo. In contrast, with the general absence of ice, there would be reduced ground albedo, and the net effect on planetary albedo and absorbed solar radiation somewhat uncertain. Water vapor and high-level clouds (hence greenhouse capacity) would have been larger, and overall the system might well have provided positive radiative feedback to whatever forced the warming in the first place. More regional assessments are unwarranted as the continental distribution was greatly different.

During the early Cretaceous, tropical drought conditions were somewhat alleviated, with the occurrence of what is interpreted from sedimentary evidence to be highly seasonal precipitation patterns [*Ziegler et al.*, 1987]. This may have been associated with a decrease in the latitudinal gradient, since the mid-Cretaceous was thought to be very warm at high latitudes [*Frakes et al.*, 1992]. Alternatively, amplified monsoons due to the continental distribution could have produced precipitation patterns completely different from those described in these experiments. During the late Cretaceous, conditions became wetter in the tropics and subtropics, perhaps indicating a continued reduction in latitudinal temperature gradient, or just a general tropical cooling. Eolian grain size evidence suggests that at the end of the Cretaceous, atmospheric circulation (i.e., eddy energy and surface winds) was as strong as in the late Cenozoic [*Janacek and Rea*, 1983; *Rea*, 1994], which would imply that the temperature gradient was generally similar to current values.

7.1.2. Tertiary climates. Through most of the Cenozoic, oxygen isotopes suggest a gradual increase in the latitudinal temperature gradient [*Frakes*, 1979]. However, during the Eocene (50 million years ago) the latitudinal temperature gradient was thought to be quite small, as indicated by the warm wet conditions at high latitudes, which featured forests and alligators in polar regions, and isotopically light marine planktonic assemblages [e.g., *Zachos et al.*, 1993, 1994; *Axelrod*, 1984; *Estes and Hutchison*, 1980]. At the same time, isotopically cool tropical temperatures have been reported [*Shackleton and Boersma*, 1981]. Of course, if the isotopic evidence is suspect for the Mesozoic, it may be for this time as well; *Adams et al.* [1990] reviewed the inconsistencies that exist between faunal and isotopic temperature estimates for the tropics. As *Barron* [1987] noted, this reduced gradient, estimated at less than one-half present-day values [*Keigwin and Corliss*, 1986] and as low as 4°C from equator to high southern latitudes [*Bralower et al.*, 1995], would have been found in the Eocence with a climate noticeably cooler than that of the Mesozoic.

A reduced temperature gradient should produce wetter conditions in the subtropics, and this does appear to have occurred. In North Africa, which by this time was approaching its current latitudinal position, areas of truly dry climate were, apparently, highly restricted [*Axelrod and Raven*, 1978], as judged from records of rainforest. Vegetation-inferred moist conditions were also found in southern Eurasia, southwestern North America, and along the west coast of South America, [*Axelrod and Raven*, 1978], regions of aridity today (although in some of these locales it is mountain induced). While some evaporite deposits (indicating aridity) were found in the subtropics, overall evaporite deposits continued to decrease from Mesozoic peaks [*Frakes*, 1979]. These results are consistent with a reduced Hadley cell intensity and temperature gradient as in experiments 2 and 4, at least from the tropics to middle latitudes, compared to the previous era. Also consistent with the reduced gradient is the estimation of a severalfold reduction in wind intensity that occurred at the time of the Paleocene-Eocene boundary [*Janacek and Rea*, 1983; *Rea*, 1994].

Results from experiment 4 are probably most applicable for the Eocene. One would anticipate increased cloud optical thickness, increased high-level clouds, and hence a larger atmospheric albedo. However, because of the likely absence of time-averaged cryospheric contributions, the ground albedo would also have been much less, implying large reductions in the planetary albedo and increased solar radiation absorption. Atmospheric water vapor and high-level cloud cover would have been greater, increasing the greenhouse capacity (and the global precipitation). In the GCM the results of such increased solar heating and increased greenhouse capacity, as in experiment 4, still do not allow the model to achieve equilibrium with the very warm sea surface temperatures. However, to maintain the very warm temperatures plus a reduced low-latitude temperature gradient, higher CO_2 levels are not sufficient, since the tropics would also warm; increased ocean heat transports also may have been required [*Barron*, 1987; *Rind and Chandler*, 1991; *Pak and Miller*, 1992; *O'Connell et al.*, 1996].

Once again, in the extratropics, eddy energy and surface winds would be reduced, shorter atmospheric waves would prevail, and precipitation would increase at the highest latitudes. Atmospheric eddy transports of moisture would likely be larger, in experiment 4 that led to a poleward atmospheric energy transport increase of 10%. Even with increased ocean heat transports, additional radiative forcing would be required to keep the high latitudes warm. This latter problem has manifested in the inability of models to maintain the apparent reduced seasonality of the Eocene in the extratropical continental interior [e.g., *Sloan and Barron*, 1992]. Increased ocean heat transports do not suffice because of the restricted geographic range of the marine influence (Plate 2). The tendency for shorter, faster-moving atmospheric waves might reduce day-to-day extremes via meridionally restricted advection patterns and less blocking events.

During the middle and later portions of the Tertiary the latitudinal temperature gradient likely increased, undoubtedly associated with the establishment of polar ice, and hydrologic indications from vegetation and soil deposits showed conditions at many latitudes approaching current distributions, especially during the last 20 million years [*Frakes*, 1979]. A gradual increase in dust size in the North Pacific is consistent with this interpretation [*Janacek and Rea*, 1983; *Rea*, 1994]. However, during the Pliocene (5–2.5 million years ago), oceanic and land temperature gradient reconstructions still indicate reductions relative to modern values [e.g., *Dowsett and Poore*, 1991; *Morley and Dworetzky*, 1991; *Groot*, 1991; *Thompson*, 1991; *Dowsett et al.*, 1994; *Wang*, 1994]. The ocean reconstructions are based on transfer functions of planktonic foraminifera assemblages, and therefore must be considered somewhat suspect, at least for the tropics. Hence the deduced reduction in the tropical temperature gradient is not so certain as that for higher latitudes.

A decreased temperature gradient with global mean tem-

peratures closer to current values would be similar to the results from experiment 2. *Dowsett et al.* [1994] summarize the available observations for ~3 million years ago. Wetter conditions prevailed in the semiarid continental interiors of North America, Africa, and Asia as well as southern Europe with drier conditions in some equatorial land regions. These results are consistent with a reduced gradient, driving a reduced Hadley circulation. The western United States was apparently consistently wetter, as found in experiment 2 (Table 4), but it is thought that topographic uplift may also have continued to affect the western United States [*Thompson*, 1991]. *Chandler et al.* [1994] in a GCM simulation, utilizing more particular boundary conditions from this time period but without a topography change, did not produce this wetness.

7.1.3. Pleistocene climates. During the Last Glacial Maximum, the *CLIMAP* [1981] reconstruction envisioned a glacial world with an increase in latitudinal temperature gradient compared with current conditions. When run in the GISS GCM, the ice age climate had a temperature gradient about 8% larger than today's. However, the gradient was not necessarily increased at all latitudes. From the tropics to 25° latitude there is essentially no change in the temperature gradient, whereas in the extratropics big increases in gradient are found.

An increase in temperature gradient would have produced a wetter tropics and drier subtropics, as in experiment 3 (Figure 5). If the gradient remained unchanged, but the climate simply cooled, it should have been wetter throughout the tropics and subtropics (experiment 3 minus experiment 1, Figure 13). The actual ice age climate appeared dry in the tropics but wetter in the subtropics. The lake level reconstructions for that time period [e.g., *Street-Perrott and Harrison*, 1984] show that only 25% of the tropical lakes studied were as high as they are currently; lake levels got relatively higher as one moved poleward, so that by 25°–35°N, most of the lakes were higher than today. From the model experiments this would be consistent with a reduction in the latitudinal temperature gradient and Hadley cell intensity, as in experiment 2. It would require more tropical cooling than existed with the *CLIMAP* [1981] sea surface temperatures. GCM experiments using the CLIMAP sea surface temperatures simulate the subtropics no wetter than today, and the simulated tropical ice age temperature was sufficiently warm, so the tropics stayed moist [*Rind and Peteet*, 1985].

A GCM experiment used Last Glacial Maximum boundary conditions but kept ocean heat transports at near current values [*Webb et al.*, 1997] (rather than the increased ocean heat convergence in the subtropical Pacific implied by the *CLIMAP* [1981] reconstruction). This run had substantial cooling in the tropics, of 5.5°C, and slightly reduced the latitudinal temperature gradient between the tropics and the subtropics. The net effect of both the colder temperatures and the reduced gradient was a weaker Hadley circulation, consistent with that implied by the hydrologic observations.

With an increase in latitudinal temperature gradient at higher latitudes, the results of experiment 3 become more relevant. Increased eddy energy and eddy transports arise from the temperature gradient change. Intensification of the Aleutian low and some weakening of the eastern portion of the Icelandic low with the increased ice age sea surface temperature gradient was reported by *Rind* [1987b] ("SST" run), consistent with the results of experiment 3. In the full ice age simulation the additional topography also produced large increases in standing eddy kinetic energy [*Rind*, 1987b].

A rapid climate change occurred circa 11,000 (^{14}C) years before the present (the Younger Dryas event). At this time the deglaciation was replaced by a sudden return within a few decades to near glacial maximum conditions, which then lasted for about 1000 years. Major questions exist concerning the extent of this change [e.g., *Rind et al.*, 1986; *Broecker*, 1994; *Peteet*, 1995]. Observations suggest that the cooling was experienced in various locales from Greenland to middle southern latitudes, including the circum-North Atlantic region, the North Pacific, equatorial Peru [*Thompson et al.*, 1995], and in some southern hemisphere middle latitudes. If the cooling was larger at high northern latitudes, it would result in an increase in the latitudinal temperature gradient, with effects as in experiments 1 and 3: increased eddy energy, intensified Aleutian low (hence reduced cooling in Alaska), strengthened subtropical highs (especially in summer, with reduced Indian monsoon), drier conditions in the subtropics, and wetter conditions in the central and eastern United States. Reduced lake levels in equatorial Africa suggest dry conditions prevailed there [*Roberts et al.*, 1993], and simultaneous reductions in methane, probably associated with reduced wetland emissions, imply general tropical drying [*Chappellaz et al.*, 1993]. This is more consistent with a reduction in the latitudinal gradient; note that just cooling, while maintaining the current gradient, produces wetter tropical conditions (Plate 4, experiment 3 minus experiment 1). In general, however, tropical and subtropical regions have not been well explored. Controversial data, either due to dating or to interpretation, exist in several relevant locations, with mixed results in others [*Peteet*, 1995]. A tentative conclusion is that the tropics cooled even more than the subtropics but probably not so much as high latitudes; the uniformity of glacial descent throughout the tropics and subtropics [e.g., *Rind and Peteet*, 1985] suggests that over land the temperature reduction was probably uniform as well.

Determining the global thermal/hydrological response for this perturbation would potentially shed light on the global response to numerous other rapid climate changes evident in the Greenland ice core. *Broecker* [1994] notes that it was unusually wet between 14,000 and 13,000 ^{14}C-years ago in the western and southeastern United States, at a time following extensive iceberg discharge into the North Atlantic ("Heinrich event"). The supposition is that this discharge led to a reduction in NADW; if so, it could then have increased the latitudinal temperature gradient, resulting in the observed wetter conditions in the southeastern United States, as in experiment 3. However, the GCM experiment increased the gradient in all ocean basins, and it raises the question of whether NADW changes can affect latitudinal gradients outside of the Atlantic Ocean. If NADW reduction was responsible for the Younger Dryas event, the observation of North Pacific cooling at that time [*Peteet*, 1995] and general instability in the North Pacific [*Thunell and Mortyn*, 1995] may imply it can affect that basin as well.

7.1.4. Holocene/recent climates. For the early portions of this time period, the climate variations were dominated by orbital forcing, with increased solar insolation during summer (e.g., 10,000–6000 years ago). Since this forcing, peaking in the subtropics, produces a latitudinal temperature gradient (and seasonality) substantially different from those investigated here, comparisons between model results and observations are unwarranted for this time.

For the little ice age period circa 1700 A.D., cooling at some relatively high latitude locations is fairly certain, especially in

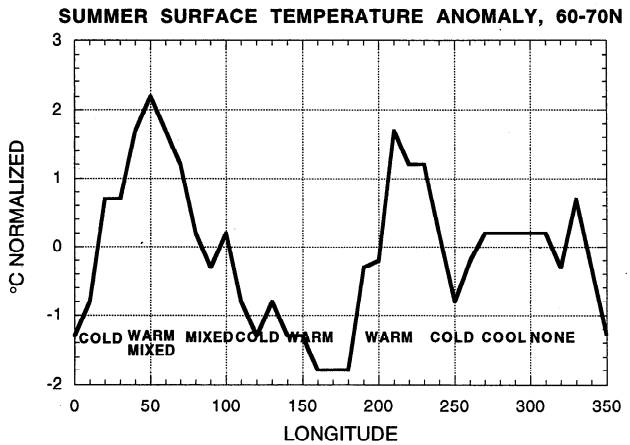

Figure 14. Summer average surface air temperature change between experiments 1 and 2 at 60°–70°N; to emphasize the longitudinal deviations, values have been normalized by subtracting out the latitudinal average change. Also shown are inferences from paleodata of observed surface air temperature changes circa 1700 A.D.

the vicinity of western Europe. At other locations, trends are more ambiguous. *Bradley* [1990] commented that in the "little ice age" period, persistent anomalies did not appear to have lasted for more than a few decades over geographically extensive areas, and only a few short cool episodes (<30 years) had anything approaching synchronicity on the hemispheric and global scale. Ice core data [e.g., *Mosley-Thompson et al.*, 1993; *Thompson et al.*, 1995] indicate that $\delta^{18}O$ records from Camp Century, Greenland, and Dunde in China show no sustained "little ice age" cooling, while records from the Huascaran and Quelccaya ice caps in Peru and from the south pole suggest prolonged cooler conditions from 1550 to 1880. The Huascaran nitrate record is also interpreted to imply reduction in Amazonian vegetation [*Thompson et al.*, 1995], presumably because of cooler and drier conditions. Hence some tropical cooling likely occurred but with the possibility that the latitudinal gradient increased in the extratropics.

One extensive cooling episode occurred around 1700 A.D. With the use of tree rings and ice core data [*Mosley-Thompson et al.*, 1993; *Jacoby et al.*, 1994; *Luckman*, 1994; *Schweingruber and Briffa*, 1994] an assessment can be made of the longitudinal variation of this effect at high northern latitudes and compared with model surface air temperature changes due to the increased gradient in experiment 1. The model predicts cold temperatures in western Europe (Figure 14) and warm values in Alaska. Inferences from the paleodata suggest a generally similar response pattern, although the comparison is not perfect. The observations could imply a cooling primarily associated with North Atlantic Deep Water production changes, affecting primarily the circum-North Atlantic. This would have the effect of increasing the latitudinal temperature gradient, and the response at other longitudes is somewhat consistent with that change. Alternatively, other forcings (e.g., solar) or natural variability may have been responsible.

For more recent times we can make a more direct assessment of what has happened to the latitudinal temperature gradient, using instrumental records. Figure 15 is the change in the observed annual surface air temperature gradient between the tropics and the polar region (data from the GISS web page, courtesy J. Hansen). During the 1930s the latitudinal gradient decreased. This would be expected, from the results in Figure 13 (experiment 2 minus experiment 1) to result in drying conditions in the United States, which is consistent with this being the "dust bowl era." *Rind and Chandler* [1991] suggested that it may have resulted from an increase in ocean heat transports, like the forcing mechanism in experiment 2.

During the 1980s the gradient was generally increased; warmer tropical temperatures occurred beginning in 1976 in the equatorial Pacific, but as shown by *International Panel on Climate Change* (*IPCC*) [1995], equatorial temperatures increased at other longitudes as well. One feature of increased gradients in the model in experiment 1 is the intensification of northward flow and warming in Alaska due to a deeper North Pacific cyclone, with relatively colder conditions over Greenland, and then warmer temperatures again in Asia. This temperature pattern is what was observed during the 1980s [e.g., *IPCC*, 1995]. The Alaskan component has previously been related to an increase in temperature gradient in the Pacific (at least up to 45°N) associated with increased El Niños [*Trenberth*, 1990; *Lau*, 1997]. In the model it arises from the impact the temperature gradient has on the planetary longwave pattern in the atmosphere, with increased gradients amplifying the prevailing troughs. In contrast, the 1988 United States drought has been related to the La Niña of that year [*Palmer and Brankovic*, 1989], which has the effect of decreasing the gradient, consistent with the results in experiment 2.

Another pattern which accompanies an increased gradient is that of drying in the Sahel (Table 4). The Sahel droughts of the 1980s and wetter conditions in the 1950s [*Folland et al.*, 1986], when the observed gradient change was negative, also agree with the results from experiments 1 and 2. Of course, the real world changes may be affected by more local conditions as well; the comparisons here are simply to emphasize that they would be expected from an increased gradient and are therefore consistent with the observed latitudinal gradient change.

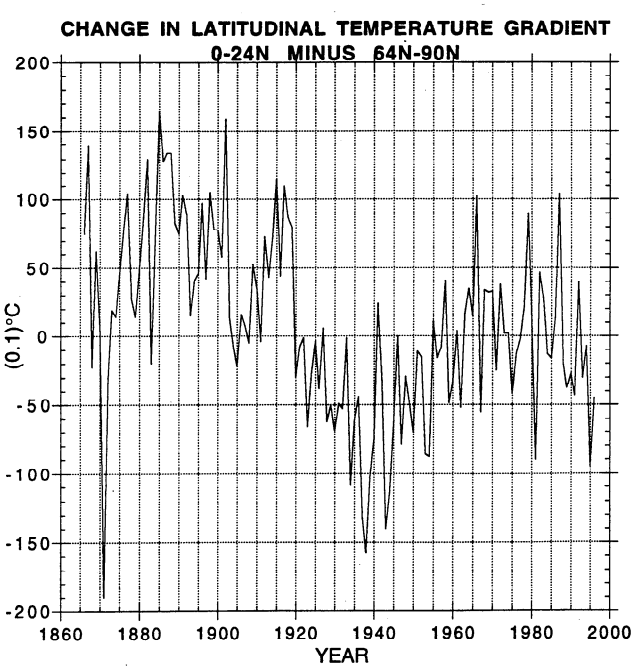

Figure 15. Change in the observed latitudinal temperature gradient, 0°–24°N minus 64°–90°N, since 1860. Data from the GISS World Wide Web Home Page, courtesy James Hansen.

It is interesting to note that many subtropical locations in both hemispheres, including large areas in Africa, India and southeast Asia, central America, southern Africa, and Australia, were relatively dry during the 1980s compared with the 1950s [*IPCC*, 1995, Figure 3.10], again consistent with this change in temperature gradient, which occurred in all ocean basins [*IPCC*, 1995].

7.2. Future Projections

What do these results imply about potential impacts of future climate change? Again, one would have to overlay the climate change itself on any latitudinal temperature gradient change, recognizing that some of the latitudinal gradient effects may be overwhelmed. The doubled CO_2 simulation reported here showed little gradient change on the annual average at most latitudes (Figure 13). Were the temperature gradient to be reduced, experiment 4 is the most likely analog, with results as in Figure 5 (drying in the tropics and lower middle latitudes, moistening in the subtropics and higher latitudes), an increased gradient would produce the opposite effects. This discussion is generally consistent with the results of *Rind* [1987a, 1988] for the doubled CO_2 simulations, which emphasized that when the tropics warm sufficiently, eddy energy remains large and tropical evaporation increases, amplifying moisture transport to the extratropics and keeping midlatitudes moist. A major caveat is the question of whether GCMs respond properly to warmer conditions, an underestimation that might lead to tropical vegetation decline even with an increased gradient [*Rind et al.*, 1997a].

Experiments with coupled atmosphere-ocean models are now being made to investigate changes in the dynamical responses of the two systems. As noted in the introduction, some models have found that the additional moisture available as climate warms leads to a freshening of the North Atlantic Ocean and a reduction in NADW production. Colder temperatures then arise at higher latitudes in the North Atlantic-European sector, increasing the latitudinal gradient in a specific longitudinal sector, as El Niño events do for the eastern Pacific sector. Some component of the model results would apply in those circumstances, presumably those in the Atlantic sector, although there is then the additional complication of changes in the longitudinal gradients between ocean basins as well. An increase in the latitudinal temperature gradient for the southern hemisphere has also been reported in coupled model experiments [*Manabe and Stouffer*, 1994; *Russell and Rind*, 1997]. In addition, the question of whether sea ice could really change rapidly in the southern hemisphere, as occurs in some models, is relevant [*Martinson*, 1993; *Rind et al.*, 1997b]; if it cannot, then little change in temperature gradient may occur in that hemisphere [*Rind et al.*, 1995, 1997b].

Can we use the results from the paleoclimate analysis to suggest what is likely with increasing CO_2? The precise relevance of past to future climates has been extensively discussed [e.g., *Webb and Wigley*, 1985; *Mitchell*, 1990; *Crowley*, 1990; *Rind*, 1993]; difficulties include the rapid nature of the projected future climate change, the different current climate background (land ice, continental configuration, ocean circulation), and questions concerning appropriate paleoclimate forcing.

This last question presents the major obstacle. The general conception is that CO_2 was higher in the Mesozoic, decreased throughout the Tertiary, and was lower during the ice ages than today [*Berner et al.*, 1983; *Owen and Rea*, 1985; *Barnola et al.*, 1987; *Caldeira and Rampino*, 1991; *Raymo and Ruddiman*, 1992]. However, we cannot be sure of the role altered CO_2 has played in past climates, compared to, for example, altered ocean heat transports [*Covey and Barron*, 1988; *Rind and Chandler*, 1991; *Chandler et al.*, 1992]. In addition, the reduced land ice in the older climates and increases during ice ages obviously influenced latitudinal temperature gradients. Even increased dust may have had an effect, by decreasing the gradient [*Overpeck et al.*, 1997].

Given these ambiguities, any conclusion as to the effects of increased CO_2 on the future latitudinal temperature gradient based on paleoclimates must be highly speculative. It appears obvious that the extratropical temperature gradient was decreased in the warmer climates and increased during the Last Glacial Maximum, but at least some of this was amplified by the land ice changes. A more modified version of this effect is likely in the future. We estimate that the early and mid-Mesozoic maintained something like the current temperature gradient from 0° to 30° latitude, while the Last Glacial Maximum had a small gradient over these same latitudes. These conclusions imply that if CO_2 was the major forcing factor, significant tropical as well as polar sensitivity to the future greenhouse forcing may be expected. (The aridity in the Mesozoic looks more like ocean heat transport effects (Figure 13, bottom), although for the ice ages, the simulations of *Manabe and Broccoli* [1985] and *Webb et al.* [1997] suggest CO_2 change was dominant, even with magnified land ice.) A reduction in poleward heat transport, as would arise from the NADW decreases seen in some coupled models, or lack of change of high-latitude sea ice in the southern hemisphere would exacerbate this situation.

In contrast, during the Tertiary, the Eocene apparently featured a reduced low-latitude temperature gradient. While the warmth of this time period may have been associated with increased CO_2, *Barron* [1991] using an ocean GCM calculated that the middle Eocene may have had deep water formed in the subtropics, hence effectively altering ocean heat transports [see also *Pak and Miller*, 1992]. Excess evaporation over restricted ocean basins could have provided highly saline water to drive this effect [*O'Connell et al.*, 1996]. During the Pliocene an apparent reduction of latitudinal temperature gradient may have been associated with increased deep water production, hence increased transports as well, rather than higher CO_2 levels [*Raymo et al.*, 1992, 1996; *Chandler et al.*, 1994]. Therefore it is not clear that these Tertiary climates automatically imply limited tropical sensitivity with increased CO_2.

The recent changes in the latitudinal temperature gradient also do not suggest a strong decrease is imminent. If it does not occur, it will reduce the likelihood that there will be midlatitude drying, a possibility raised by results such as the doubled CO_2 simulations of *Manabe and Wetherald* [1987], with a GCM that produced a strong reduction in the latitudinal temperature gradient. Droughts at lower latitudes might then be a bigger problem [*Rind et al.*, 1990].

7.3. Ice Core Results

Finally, what do these results imply about the relevance of ice core observations to global climate changes? As shown in Plate 2 and Table 4, an increase in the latitudinal temperature gradient, from altered ocean heat transports, could result in cooling over both Greenland and Antarctica without any global climate change. This possibility is perhaps more relevant for rapid climate oscillations seen in the ice cores, which may

coincide with changes in NADW formation and transports. Conceptually, at least, a decrease in poleward ocean heat transports could lead to a colder pole and warmer equator, as less heat is transported out of the equatorial region. Some evidence indicates that this pattern did prevail in the Atlantic during the Eemian (S. Lehman, personal communication, 1997), and it occurs when NADW production decreases in the coupled atmosphere-ocean model of *Russell et al.* [1995].

A change in the gradient could also change advection patterns; dust coming from Eurasia and isotopes advected in conjunction with storm tracks could both be altered with a change in temperature gradient independent of a global climate change. The results shown in Figures 9–12 indicate somewhat smaller responses in the vicinity of Greenland to the latitudinal temperature gradient, especially compared to changes that occur in the model over the North Pacific. What changes do occur show that with an increased temperature gradient, there is an increased tendency for flow to Greenland from the east or south, depending on the season, due to a weakening of the northeastern portion of the Icelandic low. This would potentially increase the Eurasian dust contribution, and with an isotope source influenced by conditions in the Norwegian Sea more so than with the current gradient might result in a confluence of both greater dust and greater apparent cooling, as has been observed [e.g., *Mayewski et al.*, 1994]. These effects would thus arise due to local advection patterns, rather than global changes. Such a deduction is highly tentative; the change in isotopic and dust advection will need to be examined in separate studies using these simulations. Nevertheless, it is consistent with the conclusion of *Mosley-Thompson et al.* [1993] that changes in ice core dust loading during the past 400 years had little global or hemispheric consistency and appeared to be dominated by local effects.

Why is the North Atlantic less sensitive to the latitudinal temperature gradient than some other regions? *Rind and Chandler* [1991] found that the western portion of the Icelandic low responded strongly to changes in the altitude of the Rockies, and *Rind et al.* [1997c] found that the eastern portion of this low responded to changes in the altitude of the Himalayas. Therefore conversely, the Icelandic low may be tightly constrained by the current topography. If this is true, then it minimizes the use of the Greenland observations to infer changes in the latitudinal temperature gradient for the current climate, or even for glacial to interglacial cycles when large changes in northern hemisphere topography occurred in ice sheet growth and decay.

Of course, the Icelandic low has varied in pressure and location, both interannually and interdecadally, without such topographic changes. *Kushnir* [1994] notes that the interannual sea level pressure variations appear to be driving the sea surface temperature changes, not the reverse. The interdecadal variations have no coherent relationship with sea surface temperatures; the ocean temperatures may be driving the atmospheric circulation into altering the ocean circulation, producing (observed) changes in sea surface longitudinal temperature gradients not allowed in this study [*Kushnir*, 1994]. Variations in sea ice also may have an effect on the Icelandic low [*Raymo et al.*, 1990].

The Antarctic ice core regions should be sensitive to advective changes associated with altered gradients (Figures 9–12). Given the range of longitudes from which ice cores are retrieved, this influence should be quantifiable, at least for separating local from latitudinal changes. For example, taking the patterns shown in Plate 2 literally, increased gradients would appear to produce warmer summer temperatures at the Vostok ice core (~115°E) than at the Byrd core (120°W), due to their locations relative to the affected offshore lows. Differences in the $\delta^{18}O$ gradient do exist among the Antarctic cores [e.g., *Bradley*, 1985], although there are many other possible causes, such as changing water vapor sources, local sea ice variations, etc. A systematic comparison of these cores might help establish patterns in the time-varying response which could be related to gradient and advective changes.

8. Conclusions

The following are some of the major conclusions of this analysis:

When the latitudinal temperature gradient increases without any global surface air temperature change, (1) Hadley circulation increases, so the subtropics dry; tropical land areas show little consistent moisture change; (2) eddy energy increases, mostly from a decrease in conversion of energy to the zonal mean flow; both surface and jet stream level winds increase; (3) atmospheric energy transports increase, but with (implicit) ocean transport decreases, there is little net transport change; (4) the Aleutian low deepens and is affected more strongly than the Icelandic low.

When the global temperature warms without much of a change in latitudinal temperature gradient (1) more moisture exists in the atmosphere at all tropospheric levels; (2) high-level clouds increase, while low-level clouds decrease; (3) over land there is less precipitation and soil moisture from 30°N to 30°S and more from 30°–60°N; (4) Hadley circulation extends slightly poleward.

When the global temperature warms and the latitudinal temperature gradient increases, (1) there is more precipitation globally, although the Hadley cell, and the pattern of rainfall/drought, is determined primarily by the latitudinal temperature gradient; (2) eddy energy changes are relatively independent of the global mean temperature, responding primarily to the latitudinal temperature gradient; (3) total atmospheric energy transport is dominated by the latitudinal temperature gradient, with the exception that latent heat transport responds to the overall warmth and moisture loading of the atmosphere; (4) the tropics are more clearly wetter, while subtropical drying is somewhat reduced.

Deductions from the results of these experiments were then applied to paleoclimate evidence to infer how the gradient may have changed in the past and how it may change in the future. It is to be emphasized that considering the quality of the paleodata and the uncertainty in model and experiment applicability, these conclusions are highly speculative.

1. The early and mid-Mesozoic climates in general may have featured a latitudinal temperature gradient between the tropics and the subtropics similar to that currently, although the climate was warmer.
2. The late Cretaceous cooled and likely maintained a large low-latitude temperature gradient.
3. In the Eocene the latitude temperature gradient was reduced.
4. During the middle and later portions of the Tertiary, latitudinal temperature gradients generally increased from prior values.
5. Pliocene latitudinal temperature gradients were still reduced relative to today.

6. During the Last Glacial Maximum, low-latitude temperature gradient was likely reduced, although possibly not over land.

7. During the Younger Dryas, there is some evidence to support a reduction in the low latitudinal temperature gradient; however, more data are needed. The same comments apply for other rapid climate oscillations during the deglaciation.

8. During the Little Ice Age the extratropical latitudinal temperature gradient may have increased even though the tropics apparently cooled.

9. The latitudinal temperature gradient has varied during the past 100 years. It was reduced from 1920 to 1960 and higher in the 1980s. Many features of observed climate trends are consistent with this variation, including recent warmer conditions in Alaska than in Greenland, warming in Asia, moisture changes in the United States, and drying in the Sahel, and the subtropics in general.

10. If the Mesozoic and Last Glacial Maximum tropical sensitivity is as large as implied here and if it was driven by CO_2 changes, then the doubled CO_2 climate may be expected to maintain a strong temperature gradient from the tropics to middle latitudes. Were NADW production to be reduced, an increase in latitudinal temperature gradient over that sector is even more likely. Precipitation decreases over middle latitudes in summer are less likely without a reduction in the latitudinal temperature gradient.

Finally, considering the relevance of polar ice core results to temperature gradient changes, (1) Greenland ice core changes might show some increase in dust and cooler conditions as a result of an increased temperature gradient; in general, however, the Icelandic low appears relatively insensitive to latitudinal temperature gradient changes, perhaps due to topographic constraints from the Rockies and Himalayas; (2) increased gradients would appear to produce warmer summer temperatures at the Vostok ice core (~115°E) than at the Byrd core (120°W), due to their locations relative to subpolar low-pressure centers.

Given the caveats inherent in the experimental setup and any modeling study, it would undoubtedly be better if paleoclimate tropical sensitivity were determined directly from paleoclimate indicators. Failing that, approaches such as this may help increase our understanding of the likely possibilities. The latitudinal temperature gradient affects all aspects of the climate system, and without understanding how it is likely to vary with the prospective climate change, very little can be said about regional predictions or implications.

Acknowledgments. Thanks go to Jean Lerner for programming support, Sukeshi Sheth for calculating the implied ocean heat transport changes, and Mark Chandler and Robin Webb for useful conversations in review. This work was supported by NOAA grant NA56GP0450. Climate modeling at GISS is supported by the NASA Climate Program Office.

References

Adams, C. G., D. E. Lee, and B. R. Rosen, Conflicting isotopic and biotic evidence for tropical sea-surface temperature during the Tertiary, *Palaeogeogr. Palaeoclimatol. Palaeoecol.*, *77*, 289–313, 1990.

Axelrod, D. I., An interpretation of Cretaceous and Tertiary biota in polar regions, *Palaeogeogr. Palaeoclimatol. Palaeoecol.*, *45*, 105–147, 1984.

Axelrod, D. I., and P. H. Raven, Late Cretaceous and Tertiary vegetation history of Africa, in *Biogeography and Ecology of South Africa*, edited by A. Werger, pp. 77–130, The Hague, 1978.

Barnola, J.-M., D. Raynaud, Y. S. Korotkevich, and C. Lorius, Vostok ice core provides 160,000-yr record of atmospheric CO_2, *Nature*, *329*, 408–414, 1987.

Barron, E. J., Eocene equator-to-pole surface ocean temperatures: A significant climate problem?, *Paleoceanography*, *2*, 729–739, 1987.

Barron, E. J., The Cenozoic ocean circulation based on ocean General Circulation Model results, *Palaeogeogr., Palaeoclimatol., Palaeoecol.*, *83*, 1–28, 1991.

Barron, E. J., and W. M. Washington, Cretaceous climate: A comparison of atmospheric simulations with the geologic record, *Palaeogeogr. Palaeoclimatol. Palaeoecol.*, *40*, 103–133, 1982a.

Barron, E. J., and W. M. Washington, Atmospheric circulation during warm geologic periods: Is the equator-to-pole surface-temperature gradient the controlling factor?, *Geology*, *10*, 633–636, 1982b.

Beck, J. W., J. Recy, F. Taylor, R. L. Edwards, and G. Cabioch, Abrupt changes in early Holocene tropical sea surface temperature derived from coral records, *Nature*, *382*, 705–707, 1997.

Berner, R. A., A. C. Lasaga, and R. M. Garrels, The carbonate-silicate geochemical cycle and its effect on atmospheric carbon dioxide over the last 100 million years, *Am. J. Sci.*, *249*, 641–683, 1983.

Bradley, R. S., *Quaternary Paleoclimatology*, 472 pp., Allen and Unwin, Winchester, Mass., 1985.

Bradley, R. S., Pre-instrumental climate: How has climate varied during the past 500 years, in *Greenhouse Gas Induced Climate Change: A Critical Appraisal of Simulations and Observations*, edited by M. Schlesinger, pp. 391–412, Elsevier, New York, 1990.

Bralower, T. J., et al., Late Paleocene to Eocene paleoceanography of the equatorial Pacific Ocean: Stable isotopes recorded at ocean drilling program site 865, Allison Guyot, *Paleoceanography*, *10*, 841–865, 1995.

Broecker, W. S., Massive iceberg discharges as triggers for global climate change, *Nature*, *372*, 421–424, 1994.

Caldeira, K., and M. R. Rampino, The mid-Cretaceous super plume, carbon dioxide and global warming, *Geophys. Res. Lett.*, *18*, 987–990, 1994.

Chandler, M., D. Rind, and R. Ruedy, A simulation of the early Jurassic climate using the GISS GCM and a comparison with the sedimentary record of paleoclimate, *Geol. Soc. Am. Bull.*, *104*, 543–559, 1992.

Chandler, M., D. Rind, and R. Thompson, Joint investigations of the middle Pliocene climate II: GISS GCM Northern Hemisphere results, *Global Planet. Change*, *9*, 197–219, 1994.

Chappellaz, J. T., Blunier, D. Raynaud, J. M. Barnola, J. Schwander, and B. Stauffer, Synchronous changes in atmospheric CH_4 and Greenland climate between 40 and 8 thousand years B.P., *Nature*, *366*, 443–445, 1993.

CLIMAP, Seasonal reconstructions of the Earth's surface at the last glacial maximum, CLIMAP Project Members, in *Map and Chart Series*, *Geol. Soc. Am.*, *MC-36*, Boulder, Colo., 1981.

Clark, D. L., Early history of the Arctic Ocean, *Paleoceanography*, *3*, 539–550, 1988.

Colinvcaux, P. A., K.-B. Liu, P. de Oliveira, M. B. Bush, M. C. Miller, and M. S. Kannan, Temperature depression in the lowland tropics in glacial times, *Clim. Change*, *32*, 19–33, 1996.

Covey, C., and E. Barron, The role of ocean heat transport in climatic change, *Earth Sci. Rev.*, *24*, 429–445, 1988.

Crowley, T. J., Are there any satisfactory geologic analogs for a future greenhouse warming?, *J. Clim.*, *3*, 1282–1292, 1990.

Dowsett, H. J., and R. Z. Poore, Pliocene sea surface temperatures of the North Atlantic Ocean at 3.0 Ma, *Quat. Sci. Rev.*, *10*, 189–204, 1991.

Dowsett, H. J., et al., Joint investigations of the Middle Pliocene climate, I, PRISM paleoenvironmental reconstructions, *Global Planet. Change*, *9*, 169–195, 1994.

Estes, R., and J. H. Hutchison, Eocene lower vertebrates from Ellesmere Island, Canadian Arctic Archipelago, *Palaeogeogr. Palaeoclimatol. Palaeoecol.*, *30*, 325–347, 1980.

Folland, C. K., T. N. Palmer, and D. E. Parker, Sahel rainfall and worldwide sea temperatures, 1901–85, *Nature*, *320*, 602–607, 1986.

Frakes, L. A., *Climates Throughout Geologic Time*, 310 pp., Elsevier, New York, 1979.

Frakes, L. A., J. E. Francis, and J. I. Syktus, *Climate Modes of the Phanerozoic*, 274 pp., Cambridge University Press, 1992.

Groot, J. J., Palynological evidence for Late Miocene, Pliocene and

Early Pleistocene climate changes in the middle U.S. Atlantic coastal plain, *Quat. Sci. Rev.*, *10*, 147–162, 1991.

Guilderson, T. P., R. G. Fairbanks, and J. L. Rubenstone, Tropical temperature variations since 20,000 years ago: Modulating interhemispheric climate change, *Science*, *263*, 663–665, 1994.

Hallam, A., A review of Mesozoic climates, *J. Geol. Soc. London*, *142*, 433–445, 1985.

Hay, W. W., E. J. Barron, and S. L. Thompson, Global atmospheric circulation experiments on an Earth with polar and tropical continents, *J. Geol. Soc.*, *147*, 749–757, 1990.

Horrell, M. A., Energy balance constraints on ^{18}O based paleo-sea surface temperature estimates, *Paleoceanography*, *5*, 339–348, 1990.

IPCC, *Climate Change 1995*, edited by J. T. Houghton, L. G. Meira Filho, B. A. Callander, N. Harris, A. Kattenberg, and K. Maskell, 572 pp., Cambridge University Press, New York, 1995.

Jacoby, G., R. D'Arrigo, and B. Luckman, Millennial and near-millennial scale dendroclimatic studies in northern North America, in *Climate Variations and Forcing Mechanisms of the Last 2000 Years*, *NATO ASI Ser.*, vol. 41, edited by P. D. Jones, R. S. Bradley, and J. Jouzel, pp. 67–84, Springer-Verlag, New York, 1994.

Janacek, T. R., and D. K. Rea, Eolian deposition in the Northeast Pacific Ocean: Cenozoic history of atmospheric circulation, *Geol. Soc. Am. Bull.*, *94*, 730–738, 1983.

Keigwin, L. D., and B. H. Corliss, Stable isotopes in late middle Eocene to Oligocene foraminifera, *Geol. Soc. Am. Bull.*, *97*, 335–345, 1986.

Kuo, H.-L., Three-dimensional disturbances in a baroclinic zonal current, *J. Meteorol.*, *9*, 260–278, 1952.

Kushnir, Y., Interdecadal variations in North Atlantic sea surface temperature and associated atmospheric conditions, *J. Clim.*, *7*, 141–157, 1994.

Lau, K.-M., J. H. Kin, and Y. Sud, Intercomparison of hydrologic process in AMIP GCMs, *Bull. Am. Meteorol. Soc.*, *77*, 2209–2227, 1996.

Lau, N.-G., Interactions between global SST anomalies and the mid-latitude atmospheric circulation, *Bull. Am. Meteorol. Soc.*, *78*, 21–33, 1997.

Lindzen, R., Some coolness concerning global warming, *Bull. Am. Meteorol. Soc.*, *71*, 288–299, 1990.

Luckman, B. H., Reconciling the glacial and dendrochronological records for the last millennium in the Canadian Rockies, in *Climate Variations and Forcing Mechanisms of the Last 2000 Years*, *NATO ASI Ser.*, vol. 41, edited by P. D. Jones, R. S. Bradley, and J. Jouzel, pp. 85–108, Springer-Verlag, New York, 1994.

Manabe, S., and A. J. Broccoli, A comparison of climate model sensitivity with data from the Last Glacial Maximum, *J. Atmos. Sci.*, *42*, 2643–2651, 1985.

Manabe, S., and R. J. Stouffer, Multiple-century response of a coupled ocean-atmosphere model to an increase of atmospheric carbon dioxide, *J. Clim.*, *7*, 5–23, 1994.

Manabe, S., and R. T. Wetherald, On the distribution of climate change resulting from an increase of CO_2 content of the atmosphere, *J. Atmos. Sci.*, *37*, 99–118, 1980.

Manabe, S., and R. T. Wetherald, Large-scale changes of soil moisture induced by an increase in atmospheric carbon dioxide, *J. Atmos. Sci.*, *44*, 1211–1236, 1987.

Manabe, S., K. Bryan, and M. J. Spelman, Transient response of a global ocean-atmosphere model to a doubling of atmospheric carbon dioxide, *J. Phys. Ocean.*, *20*, 722–749, 1990.

Martinson, D., Ocean heat and seasonal sea ice thickness in the southern ocean, *Ice in the Climate System*, NATO ASI Ser., vol. 1, edited by W. Peltier, pp. 597–609, Springer-Verlag, New York, 1993.

Mayewski, P. A., et al., Changes in atmospheric circulation and ocean ice cover over the North Atlantic during the last 41,000 years, *Science*, *263*, 1747–1751, 1994.

Mitchell, J. F. B., Greenhouse warming: Is the Mid-Holocene a good analogue? *J. Clim.*, *3*, 1177–1192, 1990.

Morley, J. J., and B. A. Dworetzky, Evolving Pliocene-Pleistocene climate: A North Pacific perspective, *Quat. Sci. Rev.*, *10*, 225–238, 1991.

Mosley-Thompson, E., L. G. Thompson, J. Dai, M. Davis, and P. N. Lin, Climate of the last 500 years: High resolution ice core records, *Quat. Sci. Rev.*, *12*, 419–430, 1993.

O'Connell, S., M. A. Chandler, and R. Ruedy, Implications for the creation of warm saline deep water: Late Paleocene reconstructions and global climate model simulations, *GSA Bull.*, *108*, 270–284, 1996.

Overpeck, J., D. Rind, A. Lacis, and R. Heady, Possible role of dust-induced regional warming in abrupt climate change during the last glacial period, *Nature*, *384*, 447–449, 1997.

Owen, R. M., and D. K. Rea, Seafloor hydrothermal activity links climate to tectonics: The Eocene carbon dioxide greenhouse, *Science*, *227*, 166–169, 1985.

Pak, D. K., and K. G. Miller, Paleocene to Eocene benthic foraminiferal isotopes and assemblages: Implications for deep water circulation, *Paleoceanography*, *7*, 405–422, 1992.

Palmer, T. N., and C. Brankovic, The 1988 U.S. drought linked to anomalous sea surface temperature, *Nature*, *338*, 54–57, 1989.

Parish, J. T., A. M. Ziegler, and C. R. Scotese, Rainfall patterns and the distribution of coals and evaporites in the Mesozoic and Cenozoic, *Palaeogeogr., Palaeoclimatol., Palaeoecol.*, *40*, 67–101, 1982.

Peteet, D., Global Younger Dryas?, *Quat. Int.*, *28*, 93–104, 1995.

Phillips, T. J., A summary documentation of the AMIP models, *PCMDI Rep. 18*, 343 pp., Lawrence Livermore Natl. Lab., Livermore, Calif., 1994.

Pollard, D., and M. Schulz, A model for the potential locations of Triassic evaporite basins driven by paleoclimatic GCM simulations, *Global Planet. Change*, *9*, 233–249, 1994.

Raymo, M. E., and W. F. Ruddiman, Tectonic forcing of late Cenozoic climate, *Nature*, *359*, 117–122, 1992.

Raymo, M. E., D. Rind, and W. F. Ruddimen, Climatic effects of reduced Arctic sea ice limits in the GISS II General Circulation Model, *Paleoceanography*, *5*, 367–382, 1990.

Raymo, M. E., D. Hodell, and E. Jansen, Response of deep ocean circulation to initiation of Northern Hemisphere glaciation (3–2 Ma), *Paleoceanography*, *7*, 645–672, 1992.

Raymo, M. E., B. Grant, M. Horowitz, and G. H. Rau, Mid-Pliocene warmth: Mid-Pliocene warmth: Stronger greenhouse and stronger conveyor, *Mar. Micropaleo.*, *27*, 313–330, 1996.

Rea, D. K., The paleoclimatic record provided by eolian deposition in the deep sea: The geologic history of wind, *Rev. Geophys.*, *32*, 159–195, 1994.

Rind, D., The dynamics of warm and cold climates, *J. Atmos. Sci.*, *43*, 3–24, 1986.

Rind, D., The doubled CO_2 climate: Impact of the sea surface temperature gradient, *J. Atmos. Sci.*, *44*, 3235–3268, 1987a.

Rind, D., Components of the ice age circulation, *J. Geophys. Res.*, *92*, 4241–4281, 1987b.

Rind, D., The doubled CO_2 climate and the sensitivity of the modeled hydrologic cycle, *J. Geophys. Res.*, *94*, 5385–54512, 1988.

Rind, D., Paleoclimate: Puzzles from the tropics, *Nature*, *346*, 317–318, 1990.

Rind, D., How will future climate changes differ from those of the past?, in *Global Changes in the Perspective of the Past*, edited by J. Eddy and H. Oeschger, pp. 39–50, John Wiley, New York, 1993.

Rind, D., Drying out of the tropics, *New Sci.*, *146*, 36–40, 1995.

Rind, D., and M. Chandler, Increased ocean heat transports and warmer climate, *J. Geophys. Res.*, *96*, 7437–7461, 1991.

Rind, D., and J. Lerner, Use of on-line tracers as a diagnostic tool in general circulation model development, 1, Horizontal and vertical transport in the troposphere, *J. Geophys. Res.*, *101*, 12,667–12,683, 1996.

Rind, D., and J. Overpeck, Hypothesized causes of decade-to-century-scale climate variability: Climate model results, *Quat. Sci. Rev.*, *12*, 357–374, 1994.

Rind, D., and D. Peteet, Terrestrial conditions at the last glacial maximum and CLIMAP sea-surface temperature estimates: Are they consistent?, *Quat. Res.*, *24*, 1–22, 1985.

Rind, D., and W. Rossow, The effects of physical processes on the Hadley circulation, *J. Atmos. Sci.*, *41*, 479–507, 1984.

Rind, D., D. Peteet, W. Broecker, A. McIntyre, and W. Ruddiman, The impact of cold North Atlantic sea surface temperatures on climate: Implications for the Younger Dryas cooling (11 – 10 K), *Clim. Dyn.*, *1*, 3–33, 1986.

Rind, D., R. Goldberg, J. Hansen, C. Rosenzweig, and R. Ruedy, Potential evapotranspiration and the likelihood of future drought, *J. Geophys. Res.*, *95*, 9983–10,004, 1990.

Rind, D., R. Healy, C. Parkinson, and D. Martinson, The role of sea ice in $2 \times CO_2$ climate model sensitivity, 1, The total influence of sea ice thickness and extent, *J. Clim*, *8*, 449–463, 1995.

Rind, D., C. Rosenzweig, and M. Stieglitz, The role of moisture trans-

port between ground and atmosphere in global change, *Annu. Rev. Energ. Environ.*, *22*, 47–74, 1997a.

Rind, D., D. Martinson, C. Parkinson, and R. Healy, Sea ice forcing of climate change, in *Workshop on Polar Processes in Global Climate*, edited by D. Martinson, Am. Meteorol. Soc., Boston, Mass., 1997b.

Rind, D., G. Russell, and W. F. Ruddiman, The effects of uplift on ocean-atmosphere circulation, in *Global Tectonics and Climate Change*, edited by W. F. Ruddiman and W. Prell, pp. 124–147, Plenum, New York, 1997c.

Roberts, N., M. Taieb, P. Barker, B. Damnati, M. Icole, and D. Williamson, Timing of the Younger Dryas event in East Africa from lake level changes, *Nature*, *366*, 146–148, 1993.

Ronov, A. B., V. Khain, and A. N. Balukhovsy, *Atlas of Lithological-Paleogeographic Maps of the World: Mesozoic and Cenozoic of the Continents and Oceans*, 79 pp., Acad. of Sci., St. Petersburg, 1989.

Russell, G., and D. Rind, Atmosphere-Ocean response to CO_2 increase in the GISS coupled atmosphere-ocean model, *J. Geophys. Res.*, in press, 1997.

Russell, G., J. Miller, and D. Rind, A coupled atmosphere-ocean model for transient climate studies, *Atmos. Ocean*, *33*, 683–730, 1995.

Schweingruber, F. H., and K. R. Briffa, Tree-ring density networks for climate reconstruction, in *Climate Variations and Forcing Mechanisms of the Last 2000 Years*, *NATO ASI Ser.*, vol. 41, edited by P. D. Jones, R. S. Bradley, and J. Jouzel, pp. 43–66, Springer-Verlag, New York, 1994.

Shackleton, N. J., and A. Boersma, The climate of the Eocene ocean, *J. Geol. Soc. London*, *138*, 157–157, 1981.

Shine, K. P., and A. Sinha, Sensitivity of the Earth's climate to height-dependent changes in the water vapor mixing ratio, *Nature*, *354*, 382–384, 1991.

Sloan, L. C., and E. J. Barron, A comparison of Eocence climate model results to quantified paleoclimatic interpretations, *Palaeogeogr., Palaeoclimatol., Palaeoecol.*, *93*, 183–202, 1992.

Street-Perrott, F. A., and S. P. Harrison, Temporal variations in lake levels since 30,000 yr B.P.—An index of the global hydrological cycle, in *Climate Processes and Climate Sensitivity*, J. E. Hansen and T. Takashashi, pp. 118–129. AGU, Washington, D. C., 1984.

Stute, M., et al., Cooling of tropical Brazil (5-degrees-C) during the Last Glacial Maximum, *Science*, *269*, 379–383, 1995.

Sun, D. Z., and R. S. Lindzen, Distribution of tropical tropospheric water vapor, *J. Atmos. Sci.*, *50*, 1644–1660, 1993.

Thompson, L. G., E. Mosley-Thompson, M. E. Davis, P.-N. Lin, K. A. Henderson, J. Cole-Dai, J. F. Bolzan, and K.-B. Liu, Late glacial stage and Holocene tropical ice core records from Huascaran, Peru, *Science*, *269*, 46–50, 1995.

Thompson, R. S., Pliocene environments and climates in the western United States, *Quat. Sci. Rev.*, *10*, 115–132, 1991.

Thunell, R. C., and P. G. Mortyn, Glacial climate instability in the Northeast Pacific Ocean, *Nature*, *376*, 504–506, 1995.

Trenberth, K. E., Recent observed interdecadal climate changes in the Northern Hemisphere, *Bull. Am. Meteorol. Soc.*, *71*, 998–993, 1990.

Tselioudis, G., W. B. Rossow, and D. Rind, Global patterns of cloud optical thickness variation with temperature, *J. Clim.*, *5*, 1484–1495, 1992.

Tselioudis, G., A. D. Del Genio, W. Kovari, and J.-S. Yao, Temperature dependence of low cloud optical thickness in the GISS GCM: Contributing mechanisms and climate implications, *J. Clim.*, in press, 1997.

Vakhrameev, V., Main features of phytogeography of the globe in Jurassic and early Cretaceous time, *Paleontol. J.* (Eng. trans.), *2*, 123–133, 1975.

Wang, L., Sea surface temperature history of the low latitude western Pacific during the last 5.3 million years, *Palaeogeogr., Palaeoclimatol., Palaeoecol.*, *108*, 379–436, 1994.

Washington, W. M., and G. A. Meehl, Climate sensitivity due to increased CO_2: Experiments with a coupled atmosphere and ocean general circulation model, *Clim. Dyn.*, *4*, 1–38, 1989.

Webb, T., and T. M. L. Wigley, What past climates can indicate about a warmer world. In M. C. MacCracken, F. M. Luther (eds). *Projecting the Climatic Effects of Increasing Carbon Dioxide*, *Rep. DOE/ER-0237*, pp. 253–257, U.S. Dep. of Energ., Washington, D. C., 1985.

Webb, R. S., D. Rind, S. J. Lehman, R. J. Healy, and D. Sigman, Influence of ocean heat transport on the climate of the Last Glacial Maximum, *Nature*, *385*, 695–699, 1997.

Zachos, J. C., K. C. Lohmann, J. C. G. Walker, and S. W. Wise Jr., Abrupt climate change and transient climates during the Paleogene: A marine perspective, *J. Geol.*, *101*, 191–213, 1993.

Zachos, J. C., L. D. Stott, and K. C. Lohmann, Evolution of early Cenozoic marine temperatures, *Paleoceanography*, *9*, 353–387, 1994.

Ziegler, A. M., A. L. Raymond, T. C. Gierlowski, M. A. Horrell, D. B. Rowley, and A. L. Lottes, Coal, climate and terrestrial productivity: The present and early Cretaceous compared, in *Coal and Coal-Bearing Strata: Recent Advances*, edited by A. C. Scott, *Geol. Soc. Spec. Publ.*, *32*, 25–49, 1987.

D. Rind, NASA Goddard Space Flight Center, Institute for Space Studies, 2880 Broadway, New York, NY 10025. (e-mail: drind@giss.nasa.gov).

(Received April 10, 1997; revised October 15, 1997;
accepted December 11, 1997.)